

ผลของกำแพงศักย์แบบ EHRlich-SCHWOEBEL ต่อระบบจำลองการปลูกฟิล์มบางแบบ WOLF-VILLAIN

นายราชัญ แรงดี

วิทยานิพนธ์นี้เป็นส่วนหนึ่งของการศึกษาตามหลักสูตรปริญญาวิทยาศาสตรมหาบัณฑิต

สาขาวิชาฟิสิกส์ ภาควิชาฟิสิกส์

คณะวิทยาศาสตร์ จุฬาลงกรณ์มหาวิทยาลัย

ปีการศึกษา 2547

ISBN 974-17-7188-6

ลิขสิทธิ์ของจุฬาลงกรณ์มหาวิทยาลัย

EFFECTS OF THE EHRLICH-SCHWOEBEL POTENTIAL BARRIER ON
THE WOLF-VILLAIN MODEL SIMULATIONS FOR THIN FILM GROWTH

Mr. Rachan Rangdee

A Thesis Submitted in Partial Fulfillment of the Requirements
for the Degree of Master of Science in Physics

Department of Physics

Faculty of Science

Chulalongkorn University

Academic year 2004

ISBN 974-17-7188-6

นายราชัญ แรงดี: ผลของกำแพงศักย์แบบ EHRlich-SCHWOEBEL ต่อระบบจำลองการปลูกฟิล์มบางแบบ WOLF-VILLAIN. (EFFECTS OF THE EHRlich-SCHWOEBEL POTENTIAL BARRIER ON THE WOLF-VILLAIN MODEL SIMULATIONS FOR THIN FILMS GROWTH) อ. ที่ปรึกษา: ดร.ปัทมา ฉัตรภรณ์, จำนวนหน้า 62 หน้า. ISBN 974-17-7188-6.

ปัจจุบันมีการศึกษาถึงลักษณะความขรุขระของพื้นผิวฟิล์มบางที่ปลูกโดยวิธีโมเลกุลาร์บีมเอพิแทกซี (MBE) อย่างมากมาย แบบจำลอง Wolf-Villain (WV) ก็เป็นแบบจำลองอย่างง่ายที่ถูกเสนอขึ้นเพื่อใช้ในการศึกษาการปลูกฟิล์มบางแบบ MBE ในอุดมคติ ในแบบจำลองนี้สมมติให้มีการปล่อยอะตอมแบบสุ่มตำแหน่งลงบนวัสดุฐานรองหนึ่งมิติ อะตอมที่ตกลงมาแล้วจะมีการแพร่อย่างทันทีทันใดภายใต้ระยะที่จำกัดที่สามารถแพร่ไปได้ และอะตอมจะพยายามแพร่ไปยังตำแหน่งที่สามารถเพิ่มจำนวนพันธะให้ได้มากที่สุด เราได้ทำการศึกษาถึงสมบัติและลักษณะทางสถิติของพื้นผิวและค่าเบี่ยงเบนมาตรฐานของความสูงของฟิล์มบางที่ปลูกโดยใช้แบบจำลองนี้ พื้นผิวที่ได้มีลักษณะเป็นความขรุขระที่ไม่มี การก่อตัวของภูเขาเกิดขึ้น ค่าเบี่ยงเบนมาตรฐานของความสูงนี้ทำให้เราสามารถคำนวณค่าเอกซ์โพเนนต์ของการเติบโตคือปีตามีค่าประมาณ 0.37 และค่าเอกซ์โพเนนต์ของความขรุขระคือแอลฟามีค่าประมาณ 1.40 ซึ่งค่าเอกซ์โพเนนต์เหล่านี้สามารถช่วยให้เราบอกถึงกลุ่มสากลของแบบจำลอง WV ได้ ในทางปฏิบัติของการปลูกฟิล์มบางแบบ MBE มีกำแพงศักย์ซึ่งรู้จักกันในชื่อของกำแพงศักย์แบบ Ehrlich-Schwoebel (ES) ซึ่งกำแพงศักย์แบบ ES นี้เป็นกำแพงศักย์สำหรับอะตอมที่มีการแพร่จากตำแหน่งที่สูงกว่าลงไปยังตำแหน่งที่ต่ำกว่า ดังนั้นเราจึงสนใจทำการศึกษาถึงผลของกำแพงศักย์แบบ ES นี้ต่อแบบจำลอง WV และลักษณะพื้นผิวที่ได้จะมีความขรุขระแบบมีการก่อตัวของภูเขาขึ้นบนพื้นผิว ค่าเอกซ์โพเนนต์ของการเติบโตจะเพิ่มขึ้นในขณะนี้และมีค่าปีตาเข้าสู่ 0.5 ในการยืนยันผลเหล่านี้ได้ทำการศึกษาค่ากระแสการแพร่ของอนุภาคและฟังก์ชันความสัมพันธ์ โดยพบว่าค่ากระแสการแพร่ของอนุภาคแสดงทิศการแพร่ของอนุภาคไปในทิศทางขึ้นเขาและพบการแกว่งกวัดของฟังก์ชันความสัมพันธ์ซึ่งเป็นการยืนยันว่ากำแพงศักย์แบบ ES เป็นสาเหตุของการก่อตัวของภูเขาเกิดขึ้นบนพื้นผิวของฟิล์มบางในการศึกษาครั้งนี้

ภาควิชา...ฟิสิกส์.....ลายมือชื่อนิสิต.....
 สาขาวิชา...ฟิสิกส์.....ลายมือชื่ออาจารย์ที่ปรึกษา.....
 ปีการศึกษา...2547.....

4472382023 MAJOR PHYSICS

KEY WORDS: EHRLICH-SCHWOEBEL (ES) BARRIER / SURFACE WIDTH / PARTICLE DIFFUSION CURRENT / CORRELATION FUNCTION

RACHAN RANGDEE: EFFECTS OF THE EHRLICH-SCHWOEBEL POTENTIAL BARRIER ON THE WOLF-VILLAIN MODEL SIMULATIONS FOR THIN FILM GROWTH. THESIS ADVISOR: PATCHA CHATRAPHORN, PH.D. 62 pp. ISBN 974-17-7188-6.

Recently, there are many studies on kinetic surface roughening in Molecular Beam Epitaxy (MBE) growth. *Wolf-Villain* (WV) model is proposed as a simple limited mobility model to study ideal MBE growth. In this model, adatom is deposited at a randomly chosen site on a one dimensional substrate. The adatom then diffuses instantaneously within a finite diffusion length and it tries to maximize its coordination numbers or its bondings. We study statistical properties of the morphology and surface width (the root mean square height fluctuation) of thin films grown according to this model. The morphology is kinetically rough surface with no mound formation. The surface width gives a growth exponent $\beta \approx 0.37$ and a roughness exponent $\alpha \approx 1.40$. These exponents are used to identify the universality class of the WV model. In real MBE growth, there exists a potential barrier known as an *Ehrlich-Schwoebel* (ES) barrier. The ES barrier is a step-edge potential barrier for the adatom diffusing over a step edge from upper to lower terraces. We study the effect of the ES barrier on the WV model. It has been found that the morphology is rough with mound formation on the surface. The growth exponent in this situation increases with the value of β approaching 0.5. To confirm these results, the particle diffusion current and the correlation function are also studied. We find the uphill current and the oscillation of correlation function. These results confirm that the ES barrier is a cause of mound formation on the surface in our study.

DepartmentPhysics.....Student's signature

Field of studyPhysics.....Advisor's signature

Academic year2004.....

Acknowledgements

I would like to thank my advisor, Dr.Patcha Chatraphorn, who suggested this topic and has provided guidance and ideas during this work. She also helped me many things since I joined Condensed Matter Research Group (CMRG). I also wish to thank Dr.Sojiphong Chatraphorn for the facility on high efficiency computer for my works until completed.

I would like to thank Prof.Chandan Dasgupta for useful and motivating discussion to develop my program.

I also thank all of my friends, brothers, and sisters on CMRG for their many useful discussions and suggestions on my work. Especially, Piti Panichayunon, Suwakan Piankoranee, Soontorn Chanyawadee, and Charnwit Ruangchalermwong.

I would like to thank Associate Professor Dr.Mayuree Natenapit, Dr.Chatchai Srinitiwawong, and Dr.Burin Asavapibhop for taking times from their busy schedules to be on my thesis committee. Their comments on this thesis are also greatly appreciated.

Furthermore, I would like to thank Dr.Burin Gumjudpai for his guidance on L^AT_EX preparation and also his support, useful motivations and discussions.

I wishes to thank my friends Joy, Sueb, Pong, Au, Nil, Yot, Neng, Don, Noom, Jeab, Nim, and many friends that I cannot mention here for their helps, supports, entertainments, and encouragements.

Finally, I must be thankful to my parents and my grandmother for all of their supports, encouragements, and understanding which made me strong to get through this hard work.

This work was also supported by Naresuan University.

Table of Contents

| | |
|--|------------|
| Abstract (Thai) | iv |
| Abstract (English) | v |
| Acknowledgements | vi |
| Table of Contents | vii |
| List of Tables | ix |
| List of Figures | x |
| Chapter I Introduction and Theory | 1 |
| 1.1 Scaling | 2 |
| 1.2 Universality Class | 6 |
| 1.3 Continuum Growth Equations | 8 |
| 1.4 Particle Diffusion Current | 11 |
| 1.5 Correlation Function | 12 |
| 1.6 Overview of the Thesis | 13 |
| Chapter II Models | 16 |
| 2.1 Discrete Growth Models | 16 |
| 2.1.1 Random Deposition Model | 17 |
| 2.1.2 Wolf-Villain Model | 19 |
| 2.2 Ehrlich-Schwoebel Barrier | 19 |
| 2.3 WV Model with ES Barrier | 22 |

| | |
|---|-----------|
| Chapter III Simulation Results and Discussions | 25 |
| 3.1 Morphologies and Scaling Exponents | 25 |
| 3.1.1 Random Deposition Model | 26 |
| 3.1.2 Wolf-Villain Model | 26 |
| 3.1.3 WV-ES Model | 31 |
| 3.2 Correlation Function | 40 |
| 3.3 Particle Diffusion Current | 45 |
| 3.4 Growth Equation | 56 |
| Chapter IV Conclusions | 58 |
| References | 60 |
| Vitae | 62 |

List of Tables

| | | |
|-----|---|----|
| 1.1 | The theoretical asymptotic exponents in $d = 1+1$ and $d = 2+1$ dimensions | 10 |
| 3.1 | The particle diffusion current J in the discrete growth models . . . | 50 |

List of Figures

| | | |
|-----|--|----|
| 1.1 | The surface width plot of the system of $L = 50$ | 4 |
| 1.2 | The surface width W with varying substrate size L | 5 |
| 1.3 | The tilted substrate and the method to contributes the particle diffusion current | 14 |
| 1.4 | The oscillations of the height-height correlation function $G(r)$. . . | 15 |
| 2.1 | The flow chart of our simulation | 18 |
| 2.2 | The Random Deposition (RD) model | 20 |
| 2.3 | The diffusion rule of the Wolf-Villain (WV) model | 20 |
| 2.4 | The Ehrlich-Schwoebel (ES) barrier | 21 |
| 2.5 | The diffusion rule of the WV-ES model | 24 |
| 3.1 | The morphology and the surface width of the RD model | 27 |
| 3.2 | The growth exponent β of the WV model | 28 |
| 3.3 | The roughness exponent α of the WV model | 29 |
| 3.4 | The snapshots of the morphology created by the WV model | 30 |
| 3.5 | The mound evolutions of the WV-ES model in 1+1 dimensions . . . | 33 |
| 3.6 | The morphologies of the WV-ES model when we vary P_D from 0.0 to 1.0 | 34 |
| 3.7 | The morphologies of the WV-ES model when $P_U = P_D$ | 35 |
| 3.8 | The surface width of the WV model and the WV-ES model when $P_U = P_D$ | 36 |
| 3.9 | The morphologies of the WV-ES model | 37 |

| | | |
|------|---|----|
| 3.10 | The surface width of the system with $L = 1000$, $P_U = 1.0$ and $P_D = 0.5$ | 38 |
| 3.11 | The surface width of the WV-ES model with varies P_D and fixed P_U | 41 |
| 3.12 | The $W-t$ plot for the WV-ES model | 42 |
| 3.13 | The roughness exponent calculation in the WV-ES model | 43 |
| 3.14 | The correlation function of the RD model | 44 |
| 3.15 | The correlation function of the WV model | 46 |
| 3.16 | The correlation function of the WV-ES model | 47 |
| 3.17 | The correlation function of the WV-ES model when $P_U = P_D$. . . | 48 |
| 3.18 | The correlation function of the WV-ES model when $P_U < P_D$. . . | 49 |
| 3.19 | The particle diffusion current of the Random Deposition (RD) model | 51 |
| 3.20 | The particle diffusion current of the WV model with untilt substrate | 52 |
| 3.21 | The particle diffusion current of the WV model with vary $\tan \theta$. . . | 53 |
| 3.22 | The particle diffusion current of the WV-ES model | 54 |
| 3.23 | The particle diffusion current of the WV-ES model when $P_U = P_D$. | 55 |

Chapter I

Introduction and Theory

Recently, there are widely interests and studies on the kinetic surface roughening growth [1, 2, 3, 4, 5]. Especially, the molecular beam epitaxy (MBE) [1] thin film growth, i.e. the epitaxial growth by using MBE technique. This technique receives much interest from both experimentalists and theorists [1, 2] due to the fact that it produces very smooth films. The MBE is also a very important technique used in thin film industrials to grow high quality films. Because the rough surfaces have poor contact properties and unusable for electronic devices, scientists try to understand the behavior of the MBE growth and find a way to describe the kinetic surface roughening growth process.

In this thesis, we use computer simulations to study kinetic nonequilibrium surface roughening growth systems. The computer simulation is a convenient tool to use and it is easy to control or neglect some parameters such as substrate temperature or bonding energy depending on the aim of each study. There are many discrete growth models [1, 3, 4, 5] used to describe MBE growth processes via computer simulations. Among these many discrete growth models, we are most interested in the model that have diffusion rules which followed the *ideal* low temperature MBE growth and solid-on-solid (SOS) constraints (not allowing desorption, overhanging and bulk vacancies formation in the growing films). This model is known as the *Wolf-Villain* (WV) model [3] which will be described in more detail in the next chapter.

In real MBE growth, there is a step-edge potential barrier known as the *Ehrlich-Schwoebel* (ES) barrier [6, 7, 8]. The ES barrier prevents an atom from diffusing down to the lower terrace from the upper terrace (more details in section 2.2). We are interested in studying effects of the ES barrier in WV model. So we add the ES barrier into the WV model by modifying the model diffusion rule.

Then we find the effect of ES barrier on the WV model and compare with the original WV model.

To understand the kinetics properties we must have some background as the tools to study and understand the model. In this chapter, we will introduce some background on scaling hypothesis. This approach has become a standard tool to describe the kinetic surface roughening after Family and Vicsek [9] formulated a scaling law for the ballistic deposition (BD) model in 1985. Moreover, the concept of universality class, continuum growth equations, particle diffusion current, and correlation function are also introduced here as follow:

1.1 Scaling

In order to understand the kinetic surface roughening behavior in MBE growth, we study a quantity which can be used to describe the grown film quantitatively. That quantity is the *surface width*, W , which is the root mean square height fluctuation. It is a standard deviation of the interface height $h(x, t)$ which is a function of the substrate size L and time t , and it is defined as [1]

$$W(L, t) \equiv \sqrt{\frac{1}{L} \sum_{x=1}^N [h(x, t) - \bar{h}(t)]^2}, \quad (1.1)$$

where $h(x, t)$ is the height at the site x and at time t above the flat substrate. \bar{h} is the average height of the surface defined as

$$\bar{h}(t) \equiv \frac{1}{L} \sum_{x=1}^N h(x, t). \quad (1.2)$$

In the growth process, if the deposited particles arrive on the substrate at a constant rate, the average height of the surface increases linearly with time as

$$\bar{h}(t) \propto t. \quad (1.3)$$

If we plot the time evolution of the surface width in log-log scale, see Fig. 1.1, the surface width has two regimes separated by the time t_c which is called the

crossover time. In the first region (where $t \ll t_c$) we see that the surface width increases as a power law with time

$$W(L, t) \propto t^\beta, \quad (1.4)$$

where β is the *growth exponent*. The growth exponent β characterizes the time-dependent dynamics of the roughening process in $t \ll t_c$ regime. As seen in Fig. 1.1, the surface width W does not increase indefinitely. After the crossover time t_c , W saturates. If we plot the width of systems with different substrate size $L = 20, 30, 40, 60$ respectively, see Fig. 1.2, we find that the saturation value of the surface width, W_{sat} , increases as the substrate size L increases and it also depends on a power law

$$W_{sat}(L) \propto L^\alpha, \quad (1.5)$$

where α is called the *roughness exponent*. The roughness exponent α characterizes the roughness of the surface at $t \gg t_c$ regime. Moreover, the crossover time of the systems also increases as the substrate size increases, see Fig. 1.2. The crossover time actually depends on the substrate size L as the power law of L as

$$t_c \propto L^z, \quad (1.6)$$

where z is called the *dynamical exponent*. We can combine the above relations, Eq. (1.4) and Eq. (1.5), into a single relation as [1]

$$W(L, t) \propto L^\alpha f(t/L^z), \quad (1.7)$$

where this relation is the *scaling relation* for W . The function $f(t/L^z)$ is called the scaling function. The scaling function has two regimes. The first regime, for the small value of t/L^z ($t/L^z \ll 1$, implying $t \ll L^z$ or $t \ll t_c$) the scaling function increases as a power law as

$$f(t/L^z) \propto (t/L^z)^\beta. \quad (1.8)$$

The second regime is when $t \rightarrow \infty$ ($t/L^z \gg 1$, imply $t \gg L^z$ or $t \gg t_c$). This is the saturation regime and we have

$$f(t/L^z) \propto \text{constant}, \quad (1.9)$$

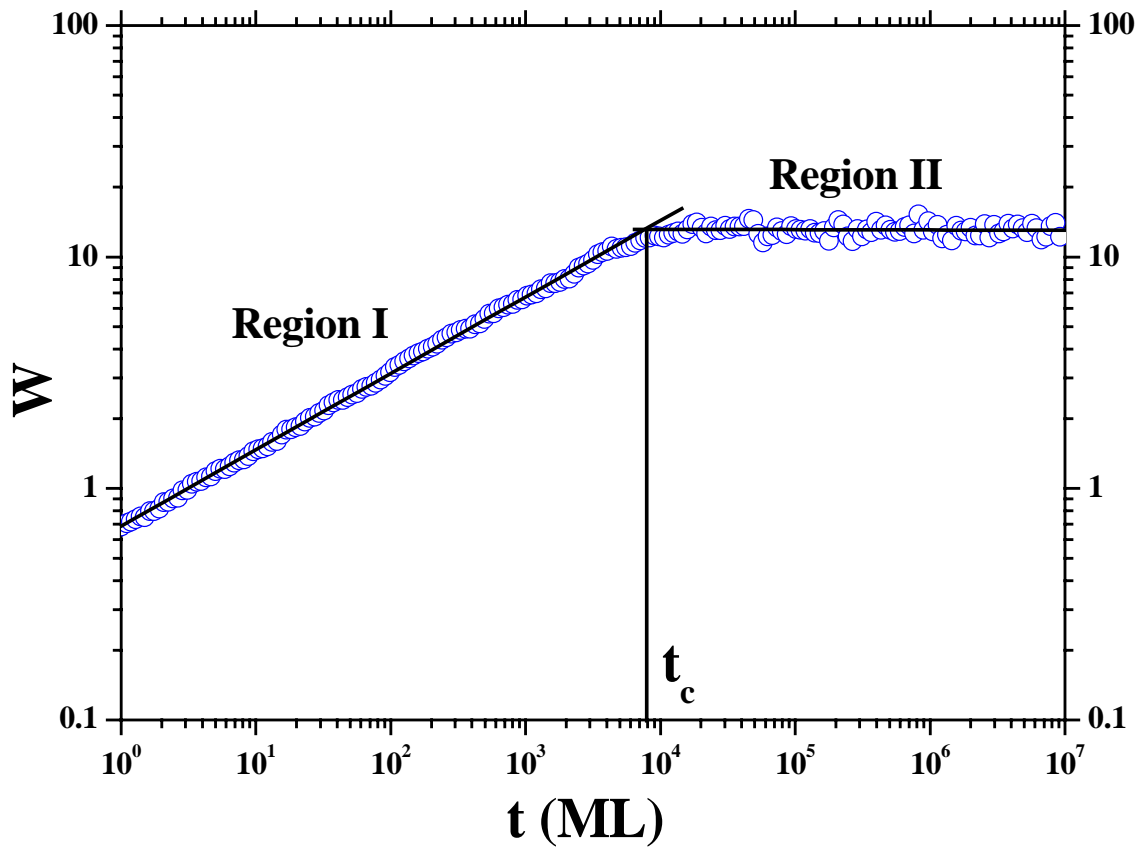


Figure 1.1: The surface width plot versus time of the system with $L = 50$. There are two regimes in this figure. The first one denoted as Region I, the surface width increases with time as a power law. The second regime, Region II, is the saturation regime that start after the crossover time t_c .

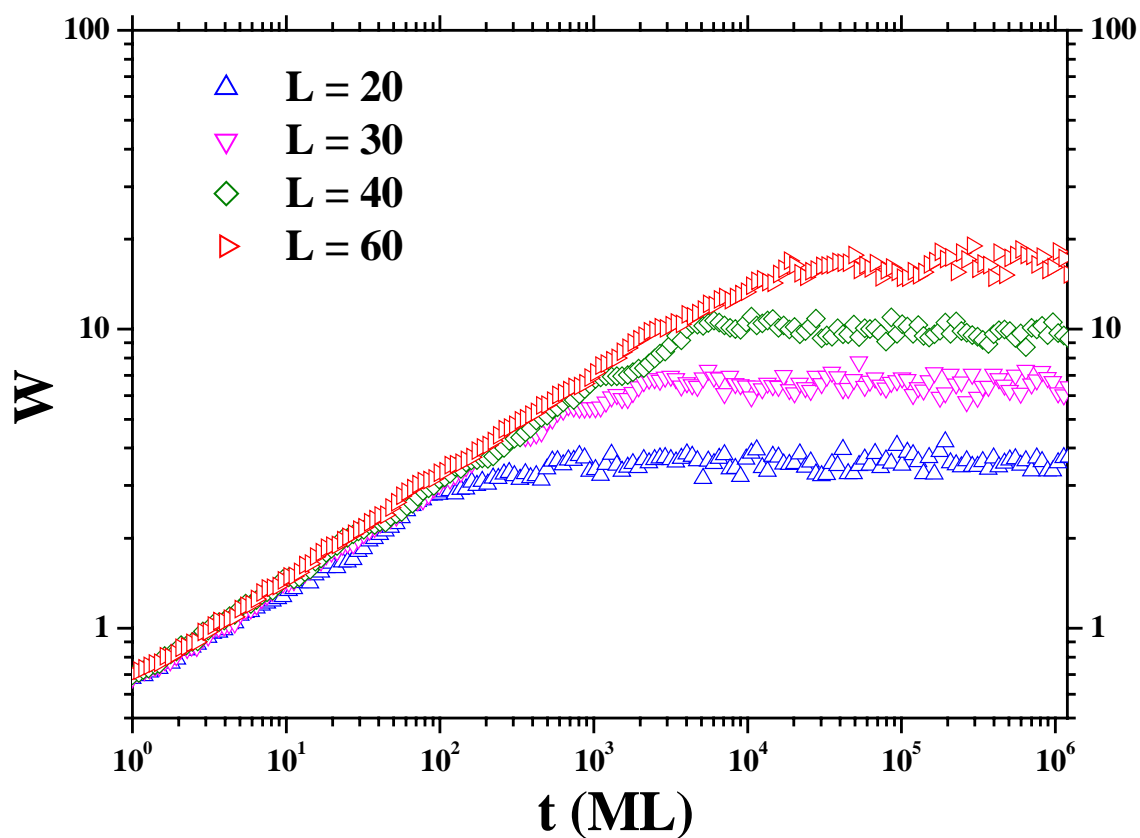


Figure 1.2: The surface width plot versus time t of the systems with different substrate size $L = 20, 30, 40, 60$ respectively. The saturation regime and the crossover time increases as the substrate size L increases.

for this limit.

The crossover time t_c is at the boundary between these two regimes, so it satisfies both Eq. (1.4) and Eq. (1.5). From this, if we approach the crossover time t_c from the left hand side we find

$$W(t_c) \propto t_c^\beta, \quad (1.10)$$

corresponding to Eq. (1.4). On the other hand, if we approach t_c from the right hand side we find

$$W(t_c) \propto L^\alpha, \quad (1.11)$$

corresponding to Eq. (1.5). From these two relations we can write

$$t_c^\beta \propto L^\alpha. \quad (1.12)$$

Substitute t_c from Eq. (1.6) we obtained

$$(L^z)^\beta \propto L^\alpha, \quad (1.13)$$

which yields

$$z = \alpha/\beta. \quad (1.14)$$

Eq. (1.14) links the three exponents α , β , z . This means there are only two independent exponents. This relation is valid for growth processes which follow the scaling relation Eq. (1.7). All of these critical exponents (α , β , z) define the *universality class* of a system, as will be discussed in more details in the next section.

1.2 Universality Class

The universality class of a growth system is defined by the set of critical exponents (roughness exponent α , growth exponent β , and dynamical exponent z). It is used to characterize the *asymptotic* (at long time, $t \rightarrow \infty$, and long distance, $x \rightarrow \infty$) properties of the kinetic roughening in epitaxial growth. In general, we need only two exponents, i.e. α and β , to define the universality class of a system because

the other exponent (z) can be represented in the form of α and β as $z = \alpha/\beta$, Eq. (1.14). There are only a few known universality classes describing asymptotic growth properties in many nonequilibrium surface growth models. There are four types [10] of universality classes for kinetic surface roughening in epitaxial growth.

1. Kardar-Parisi-Zhang (KPZ) universality

The growth process will belong to the Kardar-Parisi-Zhang (KPZ) universality class [11] if the process allows desorption, overhang, and bulk vacancies in the growing films. The critical exponents are known [11, 12] in 1+1 dimensions (one dimensional substrate) to be $\alpha = 1/2$, $\beta = 1/3$, and $z = 3/2$. In 2+1 dimensions (two dimensional substrate), the critical exponents are known approximately by numerical simulations to be $\alpha \approx 0.39$, $\beta \approx 0.24$, and $z \approx 1.61$.

2. Edwards-Wilkinson (EW) universality

The Edwards-Wilkinson (EW) universality [13] describes a growth system with no overhang, no vacancy and no desorption in the process. This type of growth is a conserve growth which is under the SOS conditions. Atoms try to diffuse down to lower terraces during EW growth. The critical exponents are exactly known in both 1+1 and 2+1 dimensions [1, 10] with $\alpha = 1/2(0)$, $\beta = 1/4(0)$, and $z = 2(2)$ in 1+1(2+1) dimensions. In 2+1 dimensions, the exponents $\alpha = \beta = 0$ predicts very smooth surfaces. The EW universality class describes the smoothest morphology in both 1+1 and 2+1 dimensions because the values of the roughness exponent (α) and the growth exponent (β) are the smallest values possible.

3. Mullins-Herring (MH) universality

The Mullins-Herring (MH) universality [14, 15] also describes a system under SOS constraints. The critical exponents in 1+1(2+1) dimensions are [10] $\alpha = 3/2(1)$, $\beta = 3/8(1/4)$, and $z = 4(4)$. The exponents α and β in MH universality are the largest values among these four universality classes. They imply that the growth morphology has the most kinetic surface roughness. The dynamical exponent $z = 4$ is a very large value. So it takes a long time for the surface width to saturate.

4. Molecular Beam Epitaxy (MBE) universality

The critical exponents for the MBE universality class are known by calculation [16], $\alpha = 1(2/3)$, $\beta = 1/3(1/5)$, and $z = 3(10/3)$ in $d = 1+1(2+1)$ dimensions.

1.3 Continuum Growth Equations

To understand the kinetic surface roughening phenomena, we want to make a connection between results obtained from the discrete growth model simulations and the continuum growth equation of motion which is used to describe the growing interfaces on the coarse-grained scale. In the continuum growth equation approach, we want to find the equation for the time derivative of the surface height $h(x, t)$ which can be written in the form [1]

$$\frac{\partial h(x, t)}{\partial t} = G(h, x, t) + \eta(x, t), \quad (1.15)$$

where $G(h, x, t)$ is a general function that depends on the interface height ($h(x, t)$), position (x), and time (t) and $\eta(x, t)$ is the fluctuations due to the random deposition process. To derive the stochastic growth equation of motion, all terms must follow symmetry principles [1, 12] of the problem:

1. Invariance under translation in time.

The growth equation must be invariant under the translation $t \rightarrow t + \delta t$ because it must not depend on where we define the origin of time. So terms that depend explicitly on t cannot be included and the survived terms are the time derivative of h , $\partial h/\partial t$, and its higher order terms because they are invariant under translation in time.

2. Invariance along the growth direction.

The growth equation must be invariant under the translation $h \rightarrow h + \delta h$ because it must be independent of where we define the level $h = 0$. So terms that depend explicitly on h cannot be included and the survived terms are the combinations of ∇h , $\nabla^2 h$, ..., $\nabla^n h$ terms.

3. Invariance along the direction perpendicular to the growth direction.

The growth equation must be invariant under the translation $x \rightarrow x + \delta x$ because it should be independent of the actual value of the position x on the substrate (where we assume that the substrate is homogeneous). So there cannot be any terms that depend explicitly on x .

4. Invariance under rotation and inversion symmetry about the growth direction.

The growth equation must be invariant under the transformation $x \rightarrow -x$. This symmetry eliminates the odd order derivative ∇h , $\nabla(\nabla h)^2$, ... terms from the growth equation. The survived terms are $(\nabla h)^2$, $\nabla^2 h$ and their combination terms.

The general form of the stochastic continuum equation after we eliminate all terms that violate any symmetry listed above is [1, 12]:

$$\frac{\partial h(x, t)}{\partial t} = \nabla^2 h + \nabla^4 h + \dots + \nabla^{2n} h + (\nabla^2 h)(\nabla h)^2 + \dots + (\nabla^{2k})(\nabla h)^{2j} + \eta(x, t), \quad (1.16)$$

where n, k, j are positive integer numbers.

Because we are interested in the asymptotic properties of the interfaces, the higher order terms are less important when comparing with the lower orders terms. We can rewrite Eq. (1.16) in the most general form for conserved epitaxial growth including all terms up to the fourth order as [2, 10, 17]:

$$\frac{\partial h}{\partial t} = \nu_2 \nabla^2 h - \nu_4 \nabla^4 h + \lambda_{22} \nabla^2 (\nabla h)^2 + \lambda_{13} \nabla (\nabla h)^3 + \eta(x, t). \quad (1.17)$$

Note that h represents the height fluctuation around the average surface height, $h = h - \bar{h}$, rather than the actual height itself. This is because we do not include a term representing the deposition flux in the equation. From the renormalization point of view, the most relevance term in Eq. (1.17) is $\nabla^2 h$ if $\nu_2 \neq 0$ [18]. This term is known as the Edward-Wilkinson (EW) term [13] and lead to the EW asymptotic universality class that we discussed in the previous section. The stochastic growth equation that includes only the EW term is

$$\frac{\partial h}{\partial t} = \nu_2 \nabla^2 h + \eta(x, t), \quad (1.18)$$

and it is generally called the EW equation [13]. If $\nu_2 = 0$, the growth Eq. (1.17) can still leads to the EW universality class because it was found [17, 18, 19] that the $\lambda_{13} \nabla (\nabla h)^3$ term is the higher order form of the EW term whenever $\lambda_{13} \neq 0$.

The extension of the EW equation to include the nonlinear second order term is proposed by Kardar, Parisi and Zhang [11]

$$\frac{\partial h}{\partial t} = \nu_2 \nabla^2 h + \lambda_2 (\nabla h)^2 + \eta(x, t), \quad (1.19)$$

where we called Kardar-Parisi-Zhang (KPZ) equation [11] and this equation lead to the KPZ universality class that describes nonconserved growth process. In general, this equation is used to describe the asymptotic behavior of nonconserved MBE growth that allows desorption, overhanging, and bulk vacancies in a growing film.

In the case when $\nu_2 = \lambda_{13} = 0$, the most relevance term is the $\nabla^2(\nabla h)^2$ term and the growth Eq. (1.17) become

$$\frac{\partial h}{\partial t} = -\nu_4 \nabla^4 h + \lambda_{22} \nabla^2 (\nabla h)^2 + \eta(x, t). \quad (1.20)$$

This is the nonlinear fourth order growth equation, which is used to describe the MBE growth [1, 2] and is called the MBE growth equation. This equation leads to the MBE universality class. The linear form of Eq. (1.20) is called the Mullins-Herring surface diffusion equation [2, 10, 14, 15, 19] which is in the form

$$\frac{\partial h}{\partial t} = -\nu_4 \nabla^4 h + \eta(x, t), \quad (1.21)$$

This equation leads to the MH universality class.

The results of the theoretically calculated asymptotic exponents [19] from Eq. (1.18) through Eq. (1.21) which corresponds with the four asymptotic universality classes are listed in Table 1.1.

| Dimensions | 1+1 | | | 2+1 | | |
|------------------------|----------|-----|---------|------------|-------------|-------------|
| | α | z | β | α | z | β |
| $\nabla^2 h$ | 1/2 | 2 | 1/4 | 0(log) | 2 | 0(log) |
| $(\nabla h)^2$ | 1/2 | 3/2 | 1/3 | ~ 0.4 | ~ 1.67 | ~ 0.24 |
| $\nabla^4 h$ | 3/2 | 4 | 3/8 | 1 | 4 | 1/4 |
| $\nabla^2(\nabla h)^2$ | 1 | 3 | 1/3 | 2/3 | 10/3 | 1/5 |

Table 1.1: The theoretical asymptotic exponents in $d = 1+1$ and $d = 2+1$ dimensions for various continuum growth equations.

1.4 Particle Diffusion Current

For our nonequilibrium growth model, we consider the model as a conserved growth model. It implies that in our growth process there are mass and volume conservation. Consequently, the surface fluctuation of the growing films can be described by the continuity, coarse-grained equation as [2]

$$\frac{\partial h}{\partial t} = -\nabla \cdot J + \eta(x, t), \quad (1.22)$$

where J is a conserved *particle diffusion current* which is parallel to the horizontal average surface height direction [2, 20]. Comparing Eq. (1.22) to Eq. (1.17), the particle diffusion current, including terms up to the fourth order, is written in the form

$$J = -\nu_2 \nabla h - \lambda_{13} (\nabla h)^3 + \nabla [\nu_4 \nabla^2 h - \lambda_{22} (\nabla h)^2]. \quad (1.23)$$

The particle diffusion current, J , in this equation is a function of the derivatives of h and a leading term is the ∇h term which is the local inclination. The current can be measured directly by the study of growth on tilted substrates [20].

To measure the particle current, we simplify the current in Eq. (1.23) and keep only the most relevance term as

$$J = -\nu_2 \nabla h, \quad (1.24)$$

where ν_2 is the EW coefficient. The growth process is started on a tilted substrate. By “tilted substrate”, it means the substrate has a non-zero inclination $\tan \theta$ and the substrate height at any position x and initial time $t = 0$ is set to be

$$h(x) = x \cdot \tan \theta, \quad (1.25)$$

for growth on one dimensional substrate (where the standard initial condition is $h(x) = 0$) as shown in Fig. 1.3. We count the numbers of diffusing atoms during growth process simulations. If an atom hops in the *uphill(downhill)* direction (represented by black arrow in Fig. 1.3), it contributes to a positive(negative) current which is shown by the red(green) arrow in Fig. 1.3(b). For atoms that do not move (stick at the deposited site) after the deposition, the current from

these atoms are zero. After the growth process is completed, we calculate the net current from the following equation:

$$J_{avg} = \frac{|J_u| - |J_d|}{n}, \quad (1.26)$$

where J_{avg} , $|J_u|$ and $|J_d|$ are the net current, the total uphill current and the downhill current in the system respectively. n is the total number of the deposited atoms. Then we consider the net current J_{avg} as follows. If the net current is positive the system is said to have an *uphill current* but if the net current is negative the system has a *downhill current*. Krug *et al.* [20] suggested that this is a powerful method to determine the true asymptotic behavior of model by determining if the EW term ($\nabla^2 h$) should be included in the continuum equation describing the model. Sign of the coefficient ν_2 in Eq. (1.17) can also be determined by this method. For a system with an *uphill* current, $j > 0$ (implying $\nu_2 < 0$), we have an unstable surface with mound formation or instabilities where as in a system with a *downhill* current, $j < 0$ (implying $\nu_2 > 0$), the surface is stable and belongs to the EW asymptotic universality class. But there is a limit to this method because there are growth models that this method does not work. One example is the Das Sarma-Tamborenia (DT) model [4, 5] that has an average zero particle diffusion current [2] which implies $\nu_2 \equiv 0$ in the model. For the case of $\nu_2 = 0$, we cannot find the true asymptotic universality class of these models by using this method. In a model with zero current, we can only conclude that the EW term is not in the continuum equation describing the model [2]

1.5 Correlation Function

In the study of thin film growth, sometimes it is difficult to distinguish a mounded surface morphology from a dynamically rough one. A useful tool that can help us distinguish between mound formation and dynamically rough is the calculation of the height-height correlation function [2, 21, 22]

$$G(\mathbf{r}) = \langle h(\mathbf{x})h(\mathbf{x} + \mathbf{r}) \rangle_x, \quad (1.27)$$

where h is the deviation of the surface height from the average height and $r = |\mathbf{r}|$ is the distance between two sites on the substrate.

If we calculate the height-height correlation function $G(r)$ and find an oscillation of $G(r)$ as a function of r , see Fig. 1.4, it implies [2, 21, 22] regular mound formation on the surface. If there is no oscillation, it implies no mound formation on the surface. Moreover, we can obtain an average mound height (H) from a $G(r)$ versus r plot through the definition [2, 23]

$$H(t) = \sqrt{G(r=0)}. \quad (1.28)$$

Conventionally, the smallest distance r which makes $G(r) = 0$, i.e. the distance of the first zero crossing of $G(r)$, is taken to be an average mound radius. The average mound radius, R , scales with growth time as [2, 23]

$$R(t) \propto t^n, \quad (1.29)$$

where $n \simeq z^{-1}$ ($= \beta/\alpha$) is the coarsening exponent which describes how the individual mound size increases in time.

1.6 Overview of the Thesis

In this chapter, we introduced the theoretical background needed for the study of far from equilibrium computational models for MBE growth. The Wolf-Villain (WV) model [3] is a simple model that we are interested in this study. It is a model with an instantaneous diffusion process. We are also interested in the effect of the step-edge potential barrier, known as the Ehrlich-Schwoebel (ES) barrier [6, 7] in the WV model. The details description of the model is presented in Chapter 2.

The results of our simulations in 1+1 dimensions of both WV model and WV model with ES barrier are presented in Chapter 3. The results of the particle current and correlation functions are also shown here. The conclusions of our work are presented in Chapter 4. In this last chapter, the true asymptotic universality class of the WV model is also discussed.

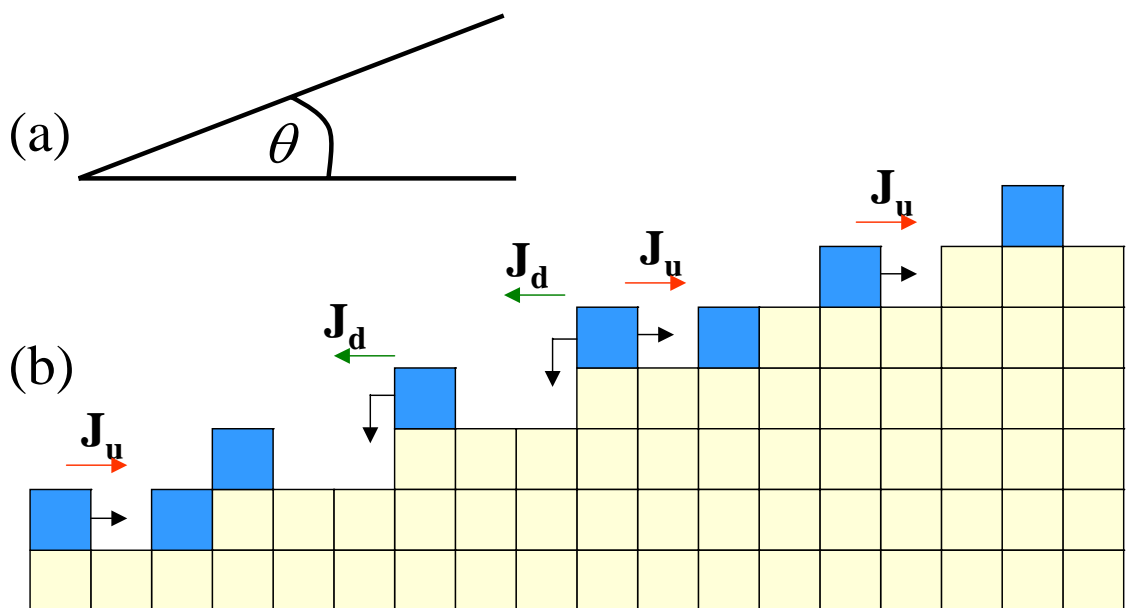


Figure 1.3: (a) The tilted substrate with the slope $\tan\theta$. (b) The method to contribute the particle diffusion current to uphill (red arrow) and downhill (green arrow) directions.

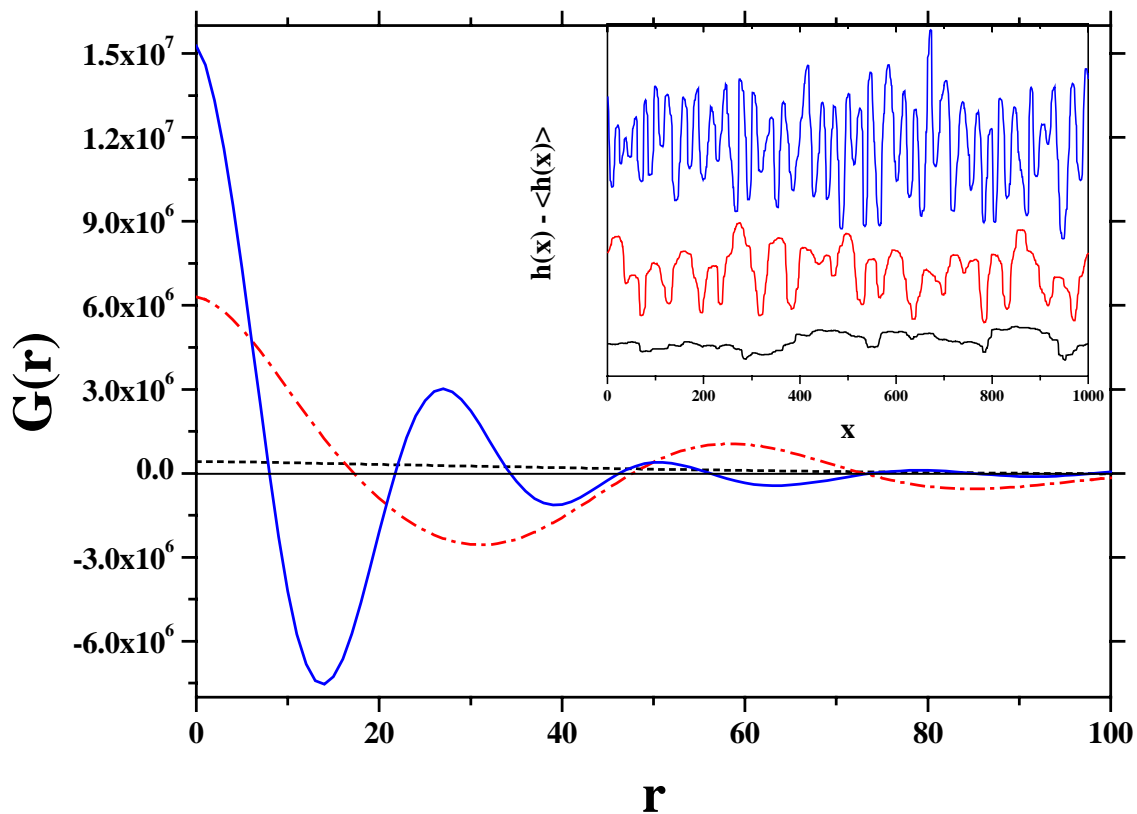


Figure 1.4: The height-height correlation function $G(r)$ shows the oscillations as a function of r . It implies mound formation on the surface (the blue line, the red dash and the dotted lines). But if there is no oscillations (the black short dash line), it implies no mound formation on the surface. Inset: The morphologies of the systems that use to calculate $G(r)$.

Chapter II

Models

Due to the increase of interest in the kinetic surface roughening growth, there are many works that try to create atomistic (discrete) nonequilibrium models to describe the growth problem and also determine essential properties and asymptotic behavior of the problem. Our work started with the simplest model known as the *Random Deposition* (RD) model. Then we deal with a more complicated model, i.e. the *Wolf-Villain* (WV) model [3]. The WV model is a simple model with the dynamical diffusion/relaxation process which we are interested and focus on in our work.

Besides studying the model, we are also interested in studying mechanisms that make the surface rough during the diffusion/relaxation process. One of these mechanisms is a potential barrier that prevents diffusing adatoms from hopping down to lower terraces. This barrier is known as the *Ehrlich-Schwoebel* (ES) barrier [6, 7, 8]. We add the ES barrier into the WV model by modifying the diffusion rules of the original WV model in order to study effects of the ES barrier on the WV model. The computational method and the diffusion rules of the models are discussed in this chapter.

2.1 Discrete Growth Models

All models we study in this work are discrete, nonequilibrium and limited mobility growth models. We assume that the models obey *ideal* low temperature MBE growth conditions. This means they are under the solid-on-solid (SOS) constraints (no desorption, no overhanging and no bulk vacancies formation on the growing surface). All of the deposited adatoms must become part of the growing film. The models are dynamical and the diffusion/relaxation process is instantaneous. In all

models studied here, the deposition of an adatom is on a randomly chosen site on a one dimensional flat substrate ($d = 1+1$). An adatom diffuses instantaneously to a selected final site and sticks there permanently (no longer move). The diffusion of a diffusing adatom is in accordance with a set of well-defined rules characterizing each model. It was found [2, 19] that the diffusion length ℓ does not have much effect on the asymptotic behavior of the growth system, so here ℓ is fixed to be unity, i.e. nearest neighbor diffusion only. In our simulations, the time t is defined through the deposition rate. In our study, one second equals to an average growth of 1 monolayer (ML) which means the deposition rate is 1 ML per second. All our simulations are done with the periodic boundary condition on the substrate, i.e. if an adatom is deposited on the site $x = L$ (L is the substrate size) and wants to diffuse to the site $x = L + 1$ then the diffusing adatom will diffuse to the site $x = 1$ instead. This periodic boundary condition prevents finite size effects in the simulations. Processes of our simulations are summarized in the flow chart as shown in Fig. 2.1.

2.1.1 Random Deposition Model

The Random Deposition (RD) model is the simplest model among many growth models. An adatom is dropped randomly above a one dimensional flat substrate and then sticks instantaneously on the deposited site with no diffusion, see Fig 2.2. This means the lateral correlation length is $\ell = 0$ for RD model. In the simulation algorithm, we choose a random site x on a flat substrate size L and increase its height $h(x)$ by one. So the surface height of the RD model grows independently and the surface of the growing film is *uncorrelated*. Since the surface height are uncorrelated, the growth front can be describe by a *Poisson distribution* [1] and we can find the exact solution [1] for the growth exponent β to be 0.5. The RD model allows the surface width to grow indefinitely with time, thus the result is no saturation in W . In this case, the roughness exponent α is not defined (that is $\alpha \rightarrow \infty$ for the RD model from Eq. (1.5)). From Eq. (1.14), the dynamical exponent z is also not defined in this model.

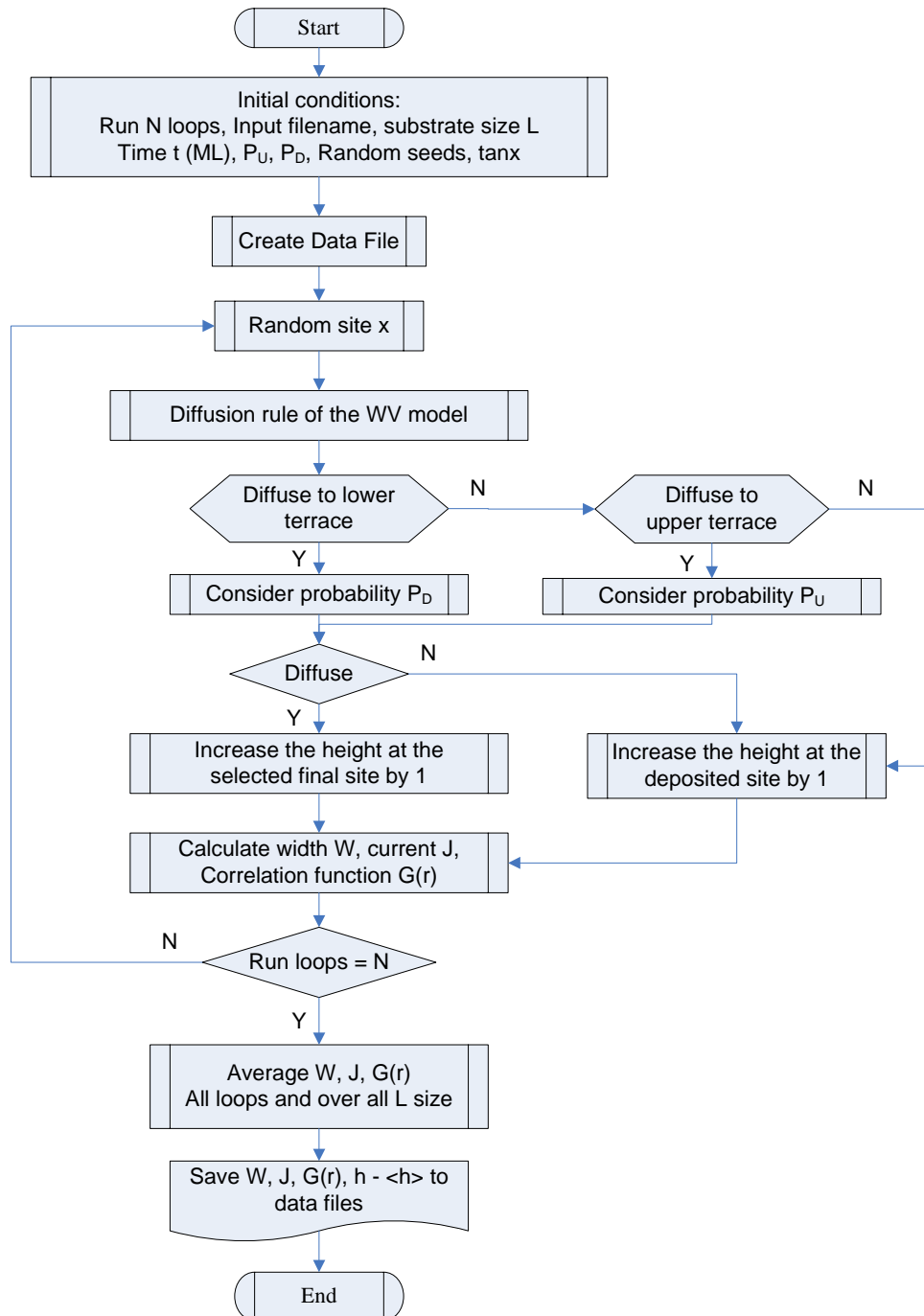


Figure 2.1: Flow chart of our simulation in all systems.

2.1.2 Wolf-Villain Model

Wolf-Villain (WV) model [3] is a simple model for kinetic surface roughening growth. It follows the MBE growth conditions and also under the SOS constraints. In the WV model, after an adatom is deposited on a randomly chosen site on a one dimensional flat substrate ($d = 1+1$), it diffuses instantaneously. In the diffusion process, the atom looks for a site within its diffusion length ℓ (for our study we set $\ell = 1$) that offers the strongest bindings. In another word, an adatom tries to increase its coordination number to the maximum value, see Fig 2.3. After an adatom finds its selected final site, it moves to that site and sticks there permanently. Then the next adatom is deposited and repeats the diffusion mechanism.

In the computational algorithm, we choose the site x randomly and then check the number of bonding at the nearest neighboring sites, $x \pm 1$, comparing with the number of bonding at the deposited site. If one of the nearest neighbor sites has higher number of bondings than at the deposited site, we increase the height at that site by one. If both nearest neighbors have higher bonding, the one with the highest coordination number is selected. If neither neighbor has larger number of bonding, we increase the height at x by one. Finally, if the number of bondings at both nearest neighboring sites (both $x \pm 1$ sites) are the same and it is more than at the deposited site, one of these sites is chosen by random (by using the random generator algorithm [24]).

2.2 Ehrlich-Schwoebel Barrier

While an adatom diffuses on the surface after being deposited on the surface, it may encounter an additional barrier called a *surface diffusion bias* [2, 20, 25]. A well known diffusion bias which leads to instability in the growing surface is the *Ehrlich-Schwoebel* (ES) barrier [6, 7, 8]. The ES barrier is a step edge potential barrier for an adatom diffusing over a step edge from upper to lower terraces, as

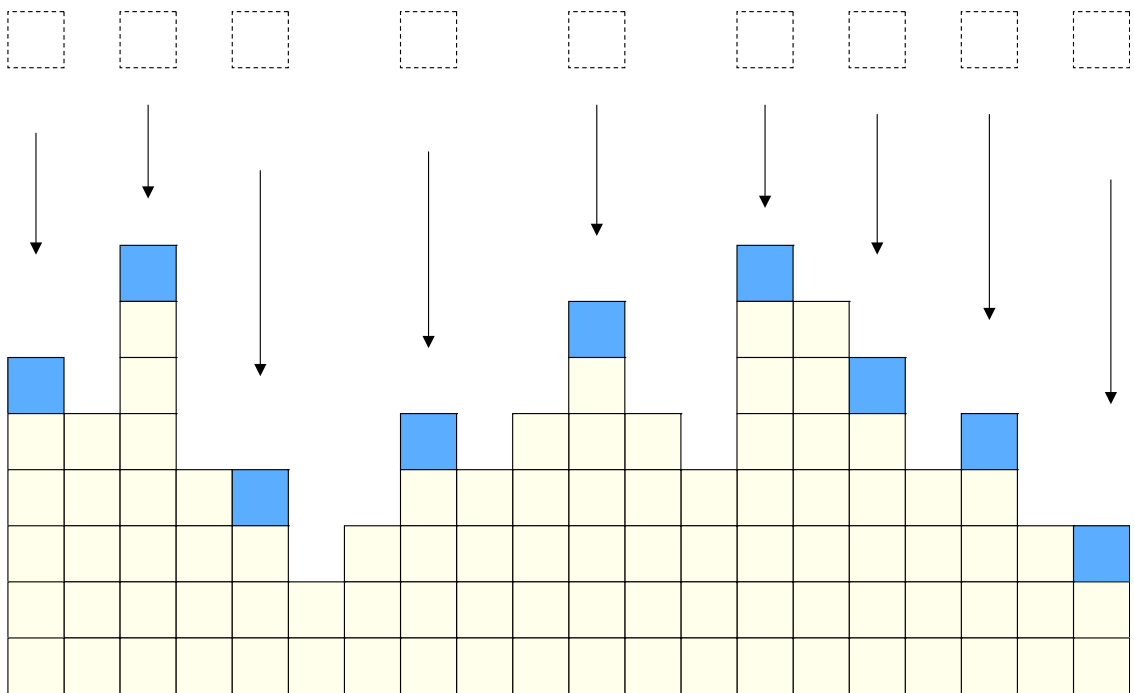


Figure 2.2: The Random Deposition (RD) model. The atoms are dropped randomly (the dash boxes) on top of the interface with no diffusion (the blue boxes).

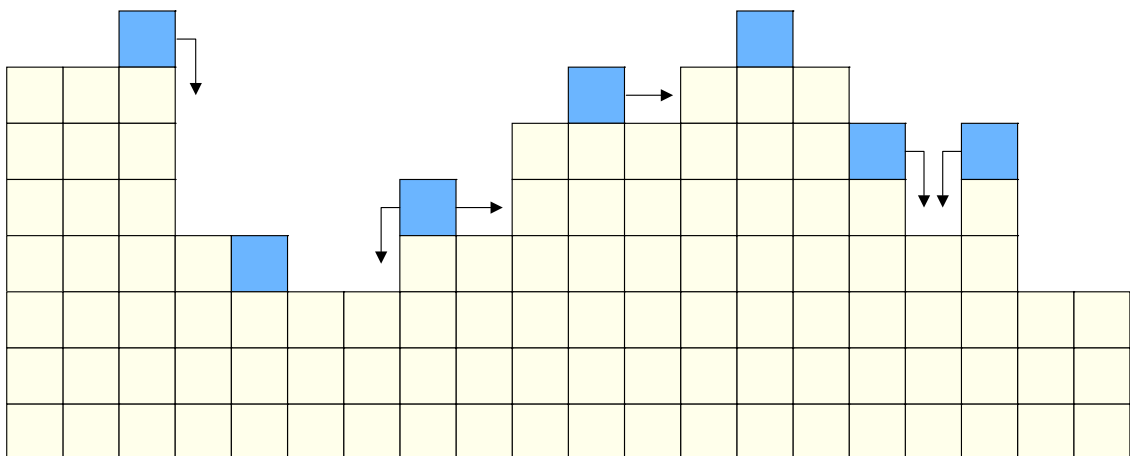


Figure 2.3: The diffusion rule of Wolf-Villain (WV) model. An adatom is deposited on a randomly chosen site on a one dimensional substrate ($d = 1+1$) and it diffuses instantaneously to increases its coordination number or its bondings.

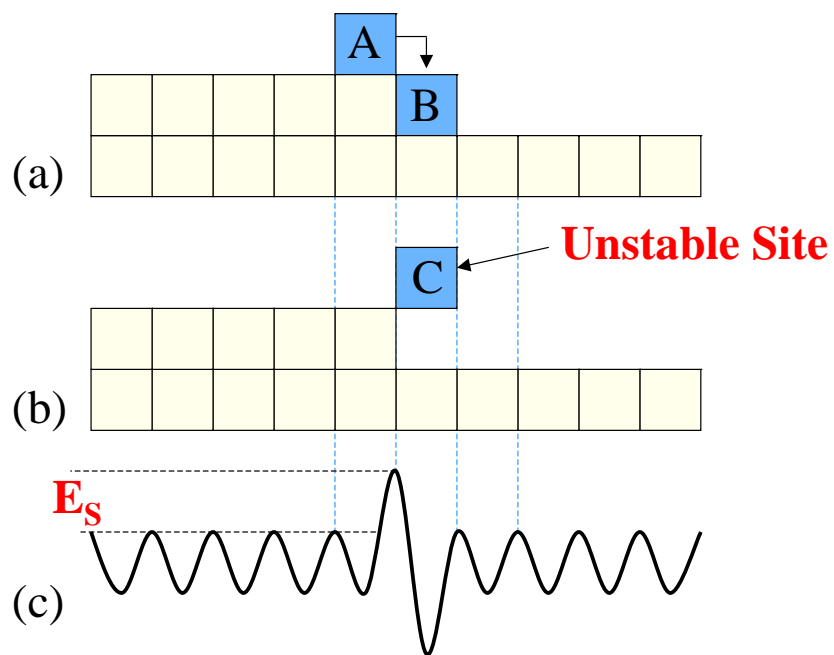


Figure 2.4: The Ehrlich-Schwoebel (ES) barrier. (a) An adatom at site A diffuses down to site B. (b) Adatom at site A must pass through an unstable site C before it arrives at site B. (c) A potential energy plot at the sites in the figures (a) and (b).

in Fig. 2.4. Since the ES barrier makes an atom more likely to attach itself to the upper terrace than the lower one, it leads to mound or pyramid type structures formation on the surface [2, 21, 22]. The mechanism of the ES barrier can be explained [1, 7, 25] as followed: While an adatom is diffusing from the upper to the lower terraces e.g. atom from site A going down to site B in Fig 2.4, it must pass through an unstable site C. At this site, there is only one bound with its next nearest neighboring site and so the atom will be very unstable at site C. This is equivalent to saying that the atom will have higher energy at site C compare to at other sites. An atom that does not have enough energy will not be able to go through site C in order to hop down to the lower terrace.

2.3 WV Model with ES Barrier

In our study, we are interested in studying effects of the ES barrier which leads to mound formation on the surface in the WV model. One of the reasons is because WV model is a good candidate [3] for studying ideal MBE growth systems and we want to understand effects of the ES barrier on the MBE growth process. Another reason is because the WV with ES barrier system possesses a conflict in the model itself. On one hand, we have the WV model which is known [3] to belong to the EW universality class. That means the system is stable with a downhill particle diffusion current [20]. On the other hand, the ES barrier is known to induce instability in a growth system [6, 7] and the particle current is uphill [20]. It is, therefore, an interesting question what type of behavior the WV model with the addition of the ES barrier will have.

In this section, we create a nonequilibrium atomistic growth model for ideal MBE growth under a surface diffusion bias (ES barrier) by implementing the ES barrier into the original WV model [3]. To add the ES barrier into the original WV model, we modified the diffusion rule of the original WV model. In Fig. 2.5, we show the modified WV model where we called WV-ES model. The diffusion rule of the WV-ES model are as follows:

1. An atom is deposited on a randomly chosen site (x) with the average rate of 1 ML per second.
2. The deposited atom looks for a better site according to the original WV diffusion rule.
3. The actual diffusion process is controlled by probabilities P_U and P_D in such a way that if the atom want to diffuse to the upper(lower) terrace, it faces the probability $P_U(P_D)$. If it cannot diffuse due to the probability, it sticks at the original deposition site.

The probabilities P_U and P_D are restricted by $0 \leq P_U, P_D \leq 1$. When $P_{U(D)} = 0$, no diffusion to the upper(lower) terrace is allowed. When $P_{U(D)} = 1$, there is no barrier in diffusion to the upper(lower) terraces. The ES barrier is implemented in our model by taking $P_D < P_U$ which makes it more likely for the adatom to attach to the upper terrace than the lower terrace. The strength of an ES barrier is controlled by the ratio P_U/P_D . If we set $P_D = P_U = 1$, our model is back to the original WV model [3]. The results of our numerical simulations, both for the WV and the WV-ES model, will be discussed in the next chapter.

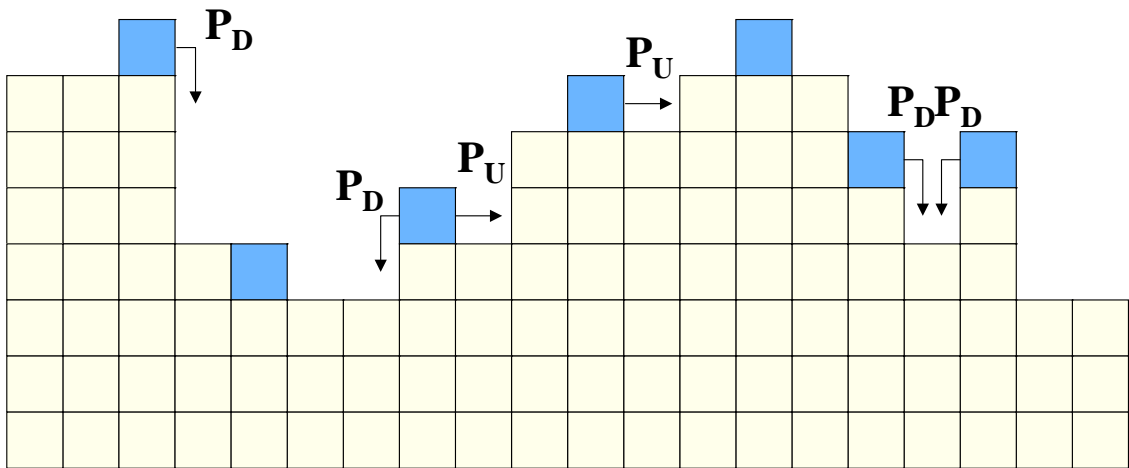


Figure 2.5: The diffusion rule of the WV-ES model. The adatom diffuses under the surface diffusion bias and it is controlled by the probabilities P_U and P_D . The ES barrier is implemented in the WV-ES model by taking the value of $P_D < P_U$.

Chapter III

Simulation Results and Discussions

As described in the previous chapter, our study is based on WV growth on one dimensional substrate ($d = 1+1$) which is flat at initial time. In fact, the one-dimensional substrate growth has never been seen [2] in experimental laboratories. But the studies of one dimensional growth systems are still important. This is because we can still gain some insight in the dynamical properties of MBE growth models while using less time in the simulations. Besides, although not an MBE growth, there exist some one dimensional interface roughening processes in real phenomena such as the snowflakes falling on the car windshield, waves clashing on the shoreline, etc. Here we study characteristic of the surface of the growing films, i.e. the *morphology*. Then we calculate the surface width W and find the exponents (α, β, z) to identify the asymptotic universality class of the WV model. Furthermore, we are interested in studying the effect of the potential barrier (ES barrier [6, 7, 8]) in WV model, the WV-ES model. The results from our simulations are shown and discussed in this chapter.

3.1 Morphologies and Scaling Exponents

In this section, we begin with our results of the simplest model (the RD model) and then focus on results of the more complicated WV model and WV-ES model later.

3.1.1 Random Deposition Model

The RD model [1] is the simplest model under the SOS constraints. In the RD model, there is no diffusion at all. The morphology and the surface width of the RD model are shown in Fig. 3.1. In Fig. 3.1(a), the morphology after depositing 10^6 ML is very rough due to the fact that each site x of the surface grows independently and the surface is uncorrelated. The surface width W plot versus time t in Fig. 3.1(b) shows that W increases indefinitely in time. The slope of this plot is the growth exponent according to Eq. (1.4). Here we have $\beta = 0.5$. The growth exponent from our simulation is in agreement with the exact solution calculated in the literature [1].

3.1.2 Wolf-Villain Model

The WV model [3] is a discrete model with very simple diffusion rules but its morphologies and scaling properties are not simple [2]. We begin by investigating the surface width of the WV model. In Fig. 3.2, we show the surface width W plot as a function of time t for a system with $L = 20,000$ lattice sites. We found the growth exponent $\beta \approx 0.37$, agreeing with previous works [2, 3, 26]. Since L is very large, we do not see any saturation in this plot.

The roughness exponent α is obtained from the plot of saturated surface width (W_{sat}) as a function of substrate size L . In Fig. 3.3, we plot the saturated width (W_{sat}) at time $t = 10^7$ ML versus the size of the substrate L , with L varying from $L = 10$ to $L = 100$. We obtained the value of the roughness exponent in one-dimensional WV model to be $\alpha \approx 1.40$. Then we calculated the third critical exponent (the dynamical exponent) z by following Eq. (1.14), $z = \alpha/\beta$. The value of the dynamical exponent z of the WV model is $z \approx 1.40/0.37 \approx 4$. All of the critical exponents (α , β , z) we obtained agree well with previous work [3] and these values correspond to the Mullins-Herring (MH) universality [14, 15] listed in Table 1.1. However, we note that many works [20, 26, 27, 28, 29] have shown that this is only a crossover behavior of the WV model. Krug *et al.* [20]

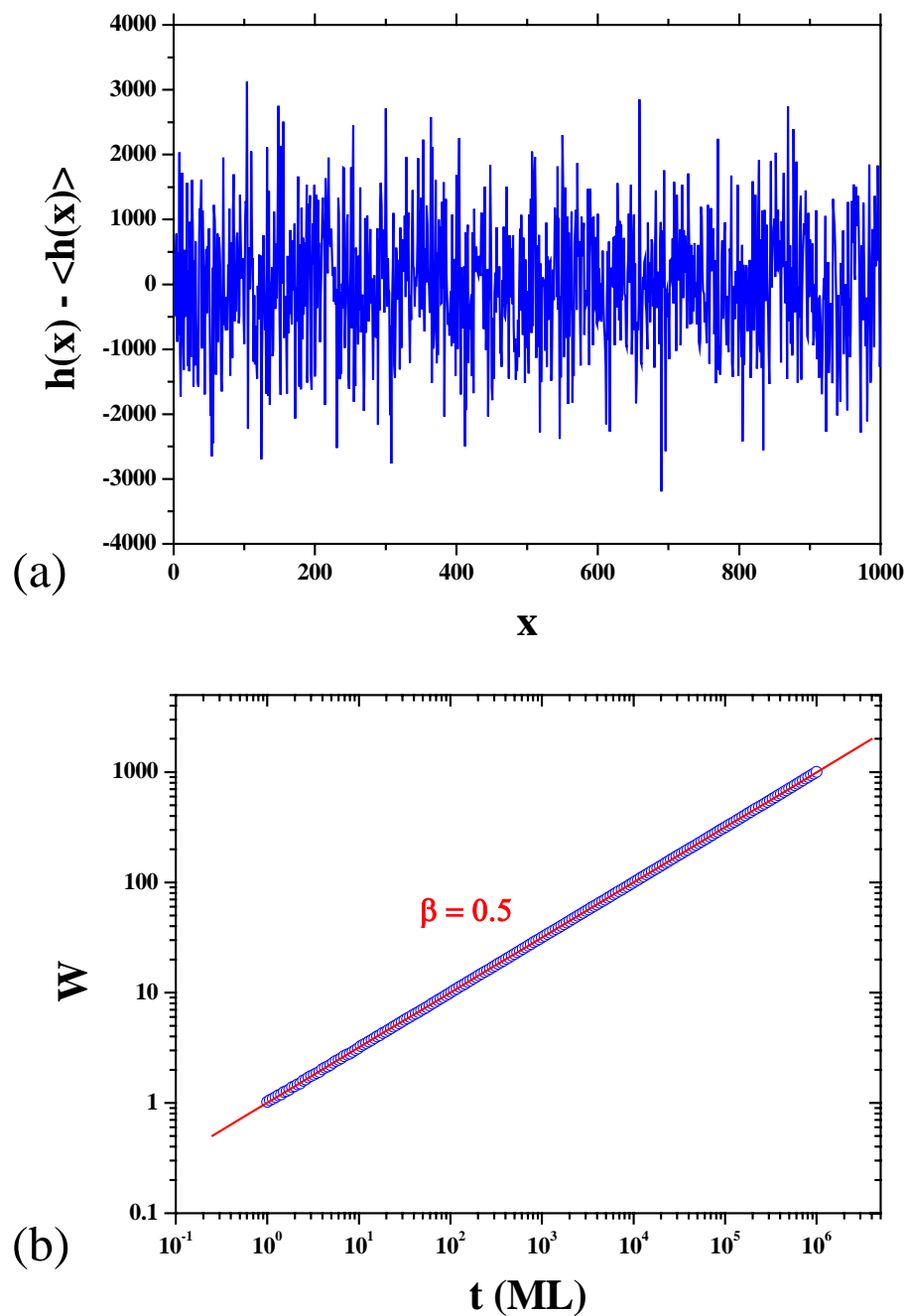


Figure 3.1: (a) The morphology and (b) the surface width of the Random Deposition (RD) model after depositing 10^6 ML on a substrate of size $L = 1000$.

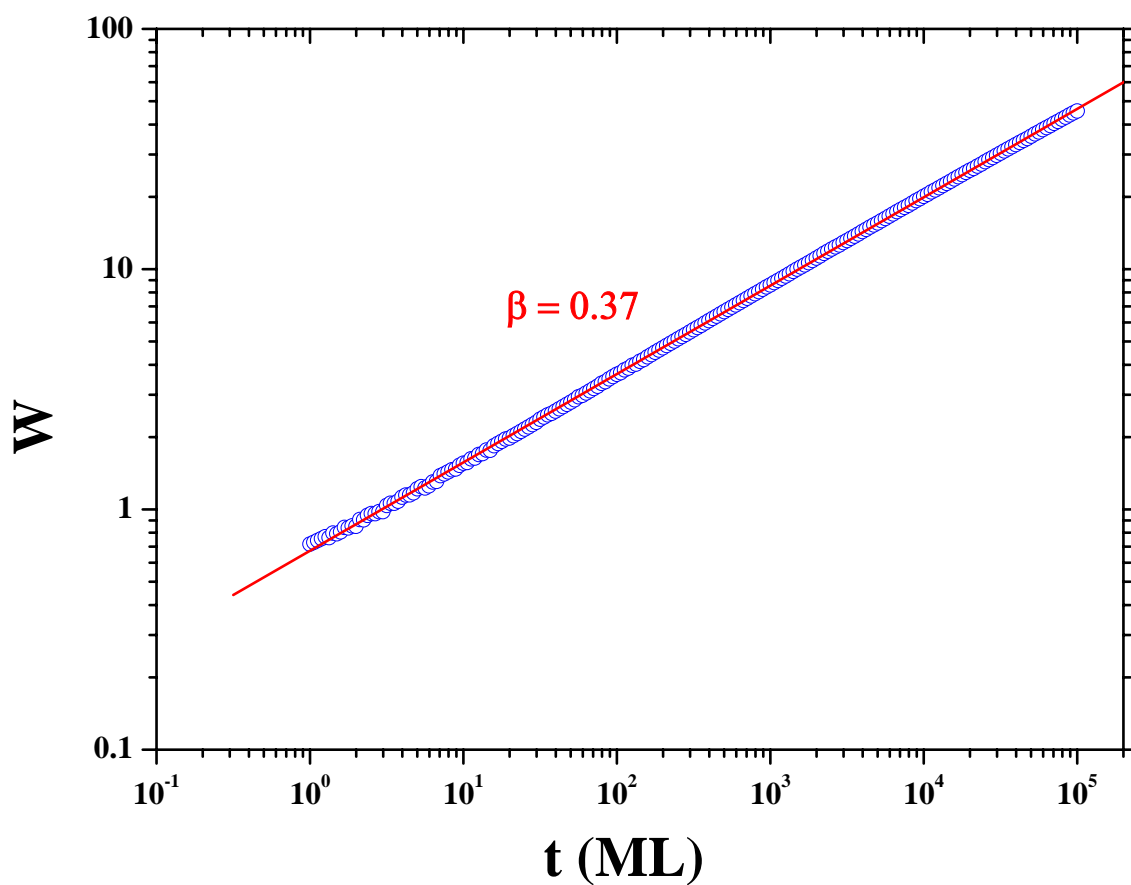


Figure 3.2: The surface width W of the WV model plot versus time t in log-log scale from the system of substrate size $L = 20,000$ at time $t = 10^5$ ML. We obtain the growth exponent $\beta \approx 0.37$ from the slope of this plot.

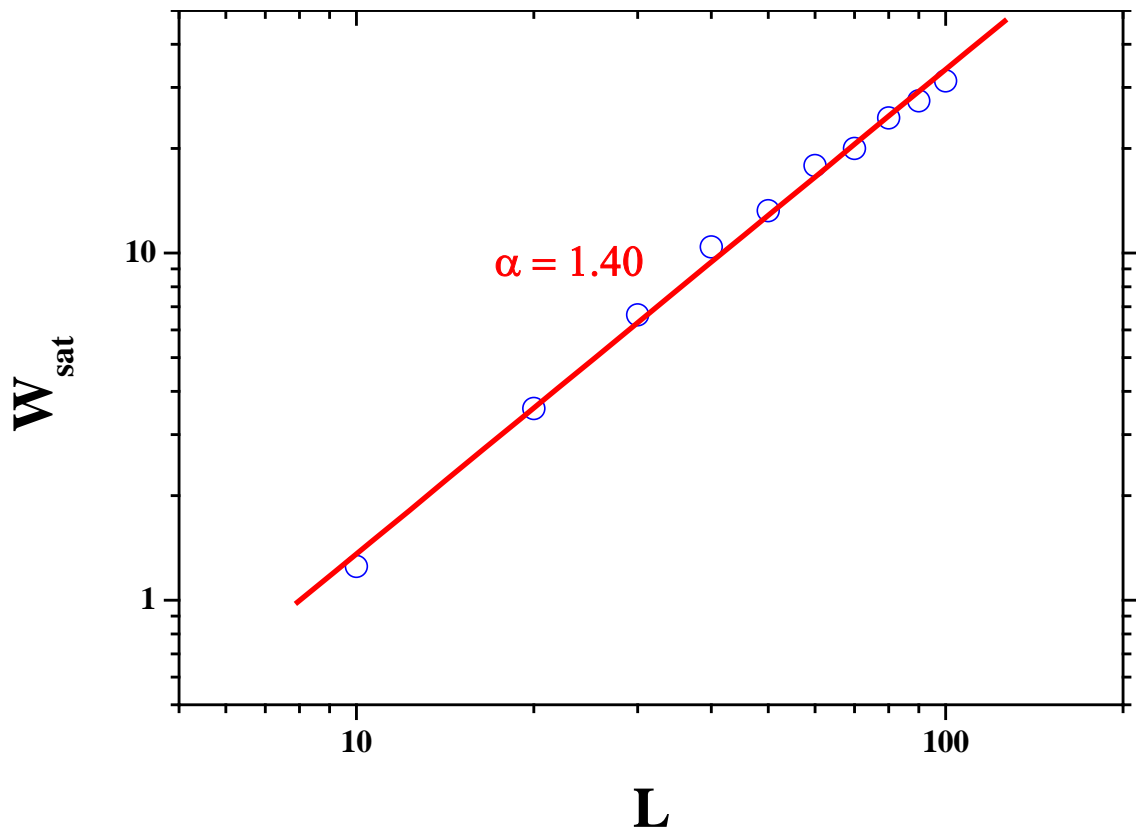


Figure 3.3: The saturate width (W_{sat}) of the WV model plot as a function of substrate size L . We simulate the systems of the substrate size $L = 10$ to $L = 100$ at time $t = 10^7$ ML. The slope of this plot is the roughness exponent $\alpha \approx 1.40$.

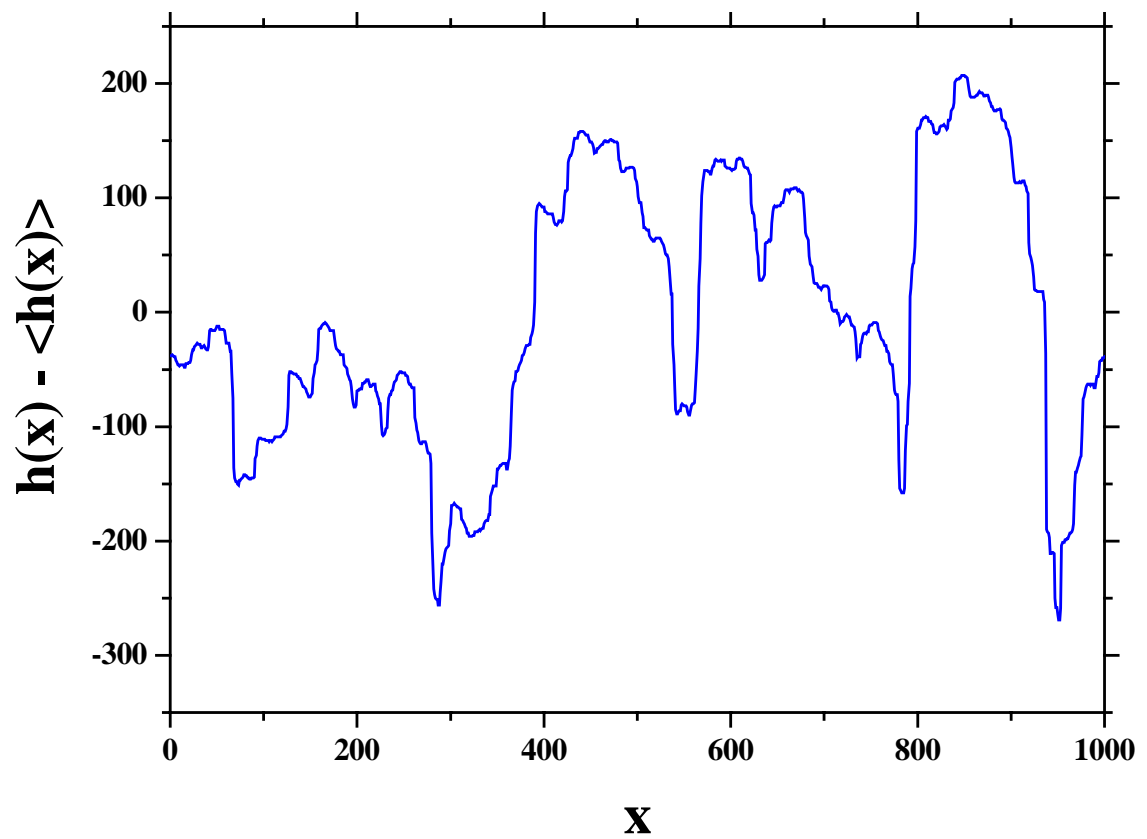


Figure 3.4: The snapshots of the morphology created by the WV model. This morphology comes from the system of substrate size $L = 1000$ and time $t = 10^6$ ML.

suggested that the true asymptotic universality class of the WV model should be the Edward-Wilkinson (EW) universality class [13]. They prove it by using the particle diffusion current calculation [20] (we will discuss this in section 3.3). In principle, if we can grow large films ($L \rightarrow \infty$) for long enough time ($t \rightarrow \infty$) we can see the crossover to the true asymptotic universality. In practical, however, due to the limitation of computers, that asymptotic time cannot be reached. So from results of the scaling exponents (α, β, z) alone, it seems to lead to the conclusion that the WV model belong to the MH universality class or the linear fourth order equation as in Eq. (1.21).

After we study the scaling behavior, we investigate the surface morphologies of this model. In Fig 3.4, we show a snapshot of the growing interface after 10^6 ML deposition. Although this is not as rough as the RD morphology (compare the minimum and maximum scales on the two plots), it seems that the WV morphology is still quite rough with deep grooves and relatively flat tops. Looking closely at this morphology we see that if we flip it upside down, the surface becomes very different from the original morphology. The new one under the $h \rightarrow -h$ transformation will have spiky peaks with shallow valleys. In other words, the up-down symmetry in the system is broken [2, 3, 19] in Fig. 3.4. This information tells us that a linear equation, such as Eq. (1.21), is not the right equation for the WV model. There must be some nonlinear terms in the equation as well. This issue will be addressed in section 3.4.

3.1.3 WV-ES Model

From the original WV model [3], we applied the effect of an ES barrier [6, 7, 8] to the original WV model by defining two probabilities P_U and P_D for adatoms attached to an upper and a lower terraces, as described in the previous chapter. The effect of the ES barrier can be seen when we set $P_D < P_U$ ($0 \leq P_D < P_U \leq 1$). In Fig 3.5 we show the time evolution of the 1+1 dimensional simulated morphology of the WV-ES model with $P_U = 1.0$ and $P_D = 0.5$. The mound formation on the surface comes from the effect of an ES barrier that deposited

adatoms cannot come down from upper to lower terraces. The mounding in the growth morphology starts after approximately 10^4 ML as can be seen in Fig. 3.5. These mound formation on the surface is sometimes referred to as an instability [2].

When we fixed $P_U = 1.0$ and vary the strength of the barrier by varying the probability P_D , we found that the surface morphologies have deeper grooves and shaper peaks in systems with stronger barrier (decreasing P_D), as in Fig. 3.6. This is due to the fact that adatoms have less chance to hop down to the lower terraces when P_D is smaller, which corresponds to stronger barrier in this situation. The average size of each mound also seems to be smaller when the barrier is stronger. When the values of P_D and P_U are equal, we found that the morphologies of the WV-ES model (Fig. 3.7) become dynamical rough (no mound formation) surfaces as found in the original WV model. This may be puzzling but it can be explained that when adatoms have equal chance to hop to upper or lower terraces, there is no bias in the model and the model reduces back to the original WV model even through $P_D, P_U < 1$. This can be confirmed by the $W-t$ plot as shown in Fig. 3.8. Of course, if we set the probabilities to be too small, it becomes difficult for atoms to hop and the morphologies in these cases are more rough, such as the system with $P_U = P_D = 0.1$ in Fig. 3.7. And when we set $P_U = P_D = 0$, we found that morphology of this case becomes the same as the morphology from the RD model [1] shown earlier in Fig. 3.1, which is totally predictable because when $P_U = P_D = 0$ atoms lose all mobility and cannot diffuse at all.

The last situation is when we set $P_D > P_U$, it was found that the morphologies are much smoother than the original WV model. This is shown in Fig. 3.9. This case corresponds with the *negative* ES barrier [30] which induces very smooth surface because most of the adatoms hop down to lower terraces and fill up the grooves.

To study the scaling behavior of the WV-ES model, we show in Fig. 3.10 the surface width W plot as a function of time t in log-log scale from a system with $L = 10^3$, $P_U = 1.0$ and $P_D = 0.5$. We found that in the early time the

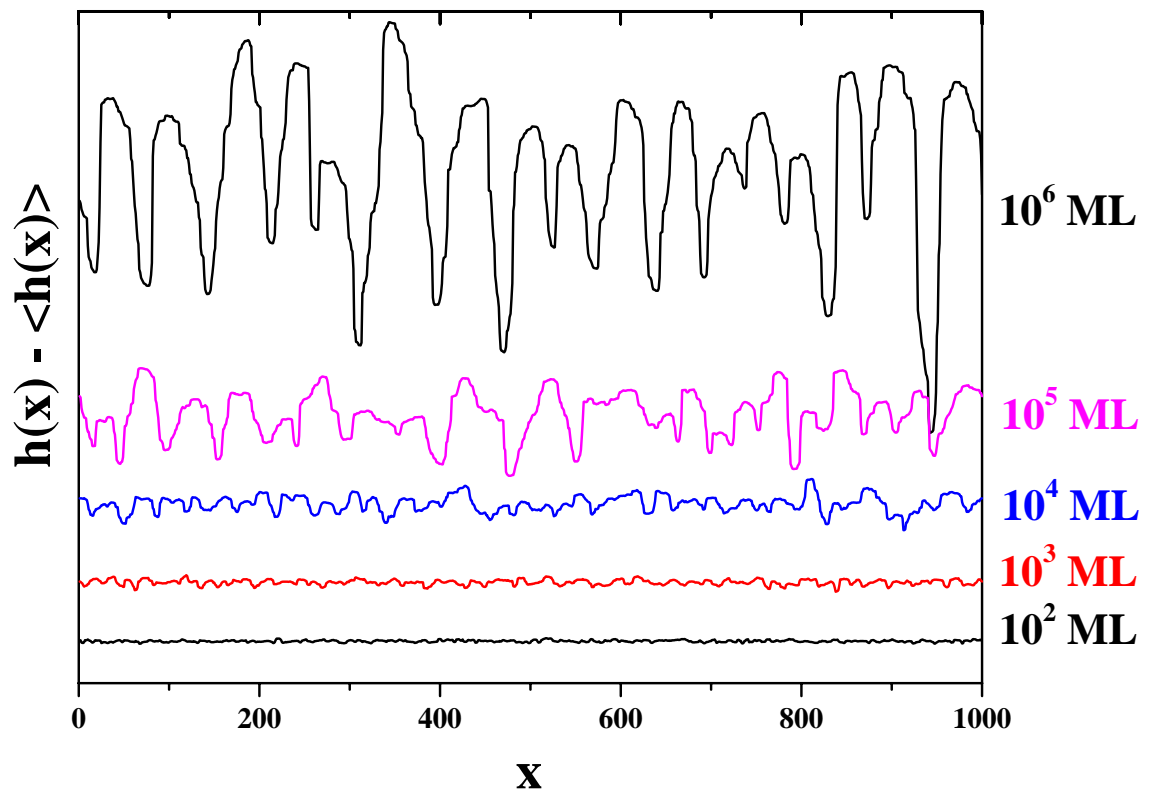


Figure 3.5: The mound evolutions of the WV-ES model in 1+1 dimensions from the systems of substrate size $L = 1000$ at time $t = 10^2 - 10^6$ ML from bottom to top. The systems are simulated with $P_U = 1.0$ and $P_D = 0.5$.

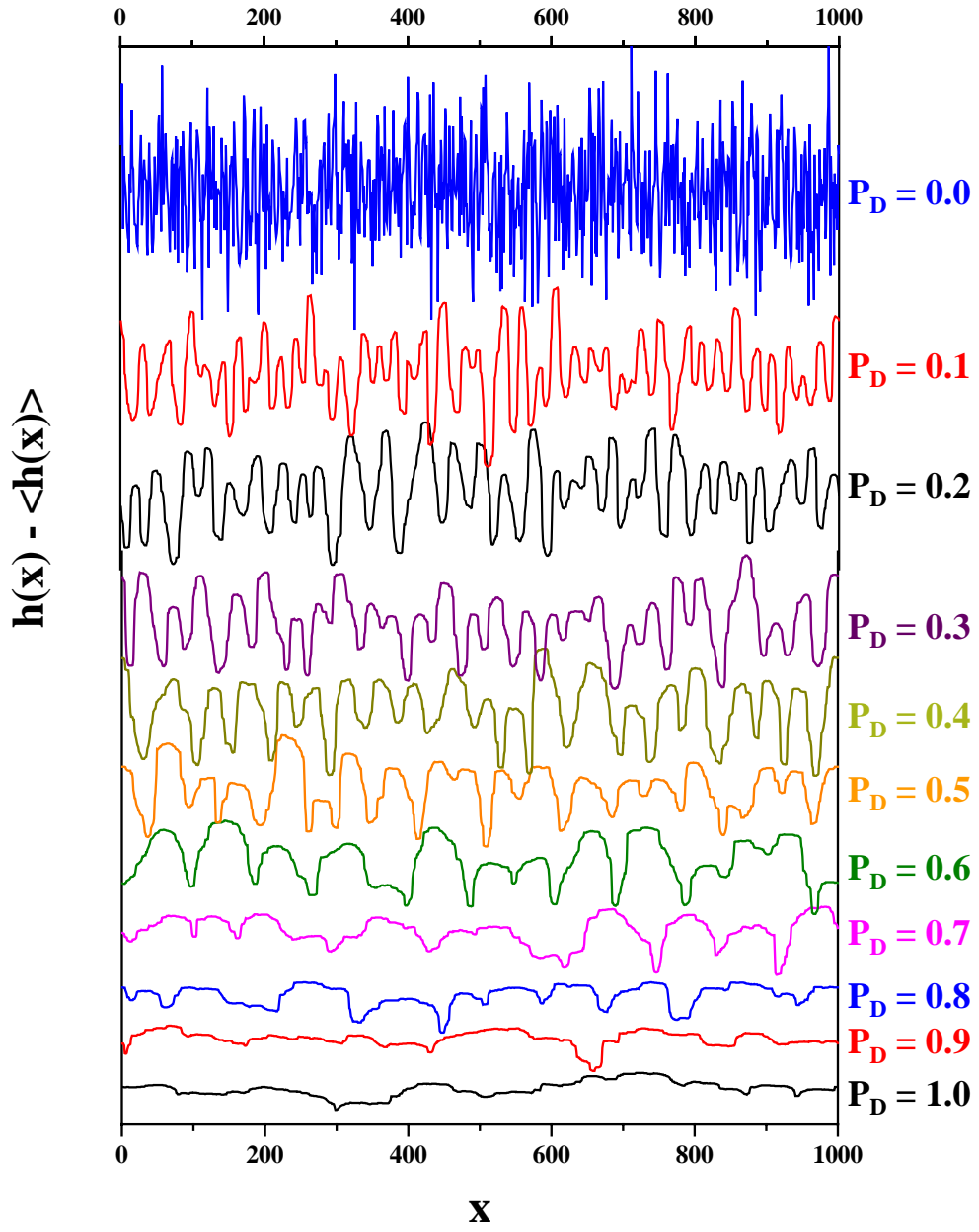


Figure 3.6: The morphologies of the WV-ES model when we vary the values of $P_D = 0.0$ to 1.0 (from top to bottom) by fixed the value of $P_U = 1.0$. We simulate the systems of substrate size $L = 1000$ at time $t = 10^6$ ML.

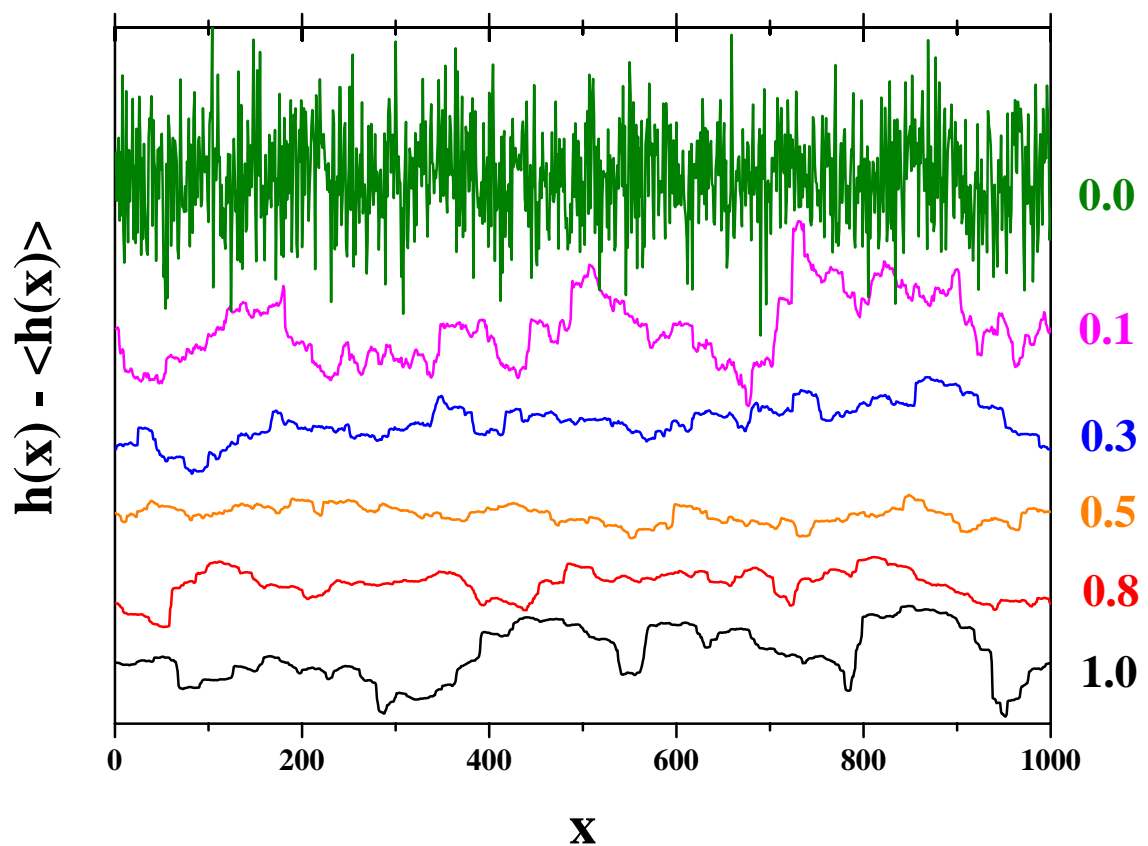


Figure 3.7: The morphologies of the WV-ES model when $P_U = P_D$. We vary the values of P_U and P_D from 1.0 to 0.0 (bottom to top). The values of P_D that equals to 1.0 and 0.0 correspond to the original WV model and RD model respectively. We simulate the systems of substrate size $L = 1000$ at time $t = 10^6$ ML.

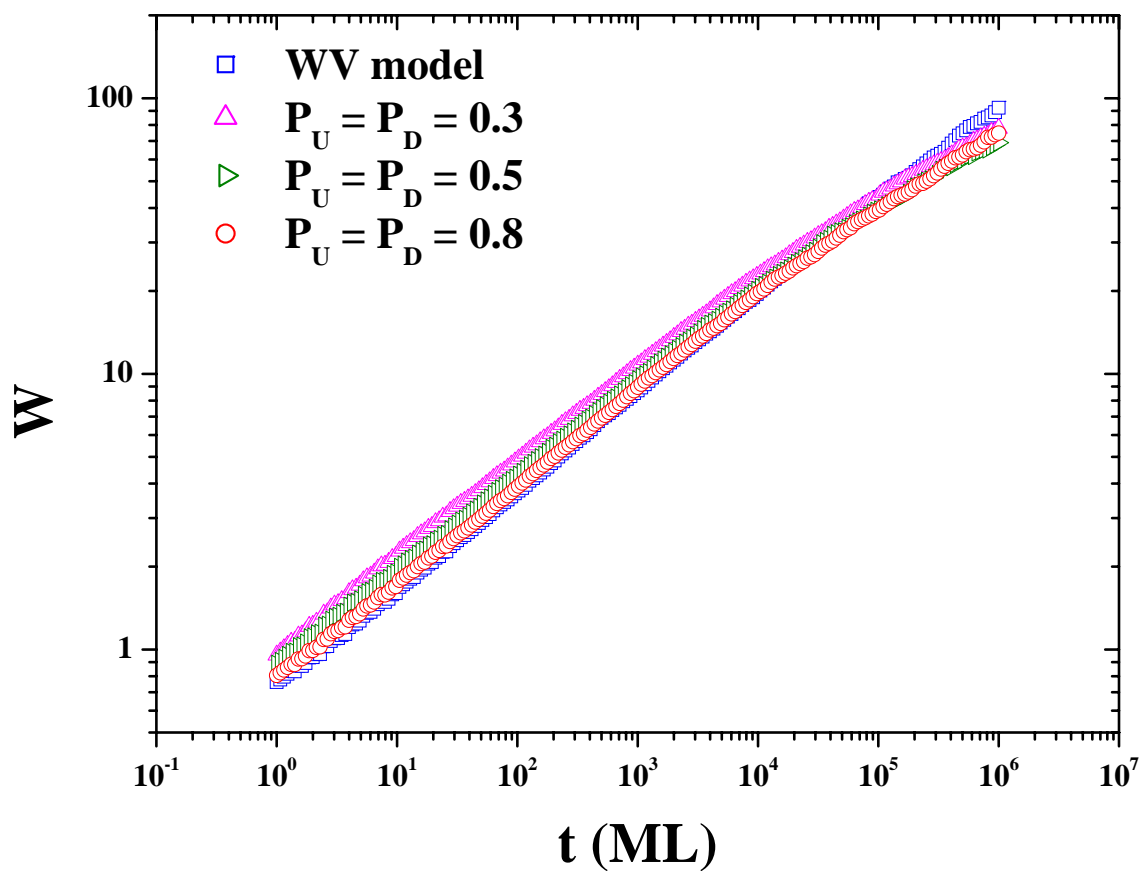


Figure 3.8: The surface width of the WV model and the WV-ES model when $P_U = P_D$. The results are from systems of substrate size $L = 1000$.

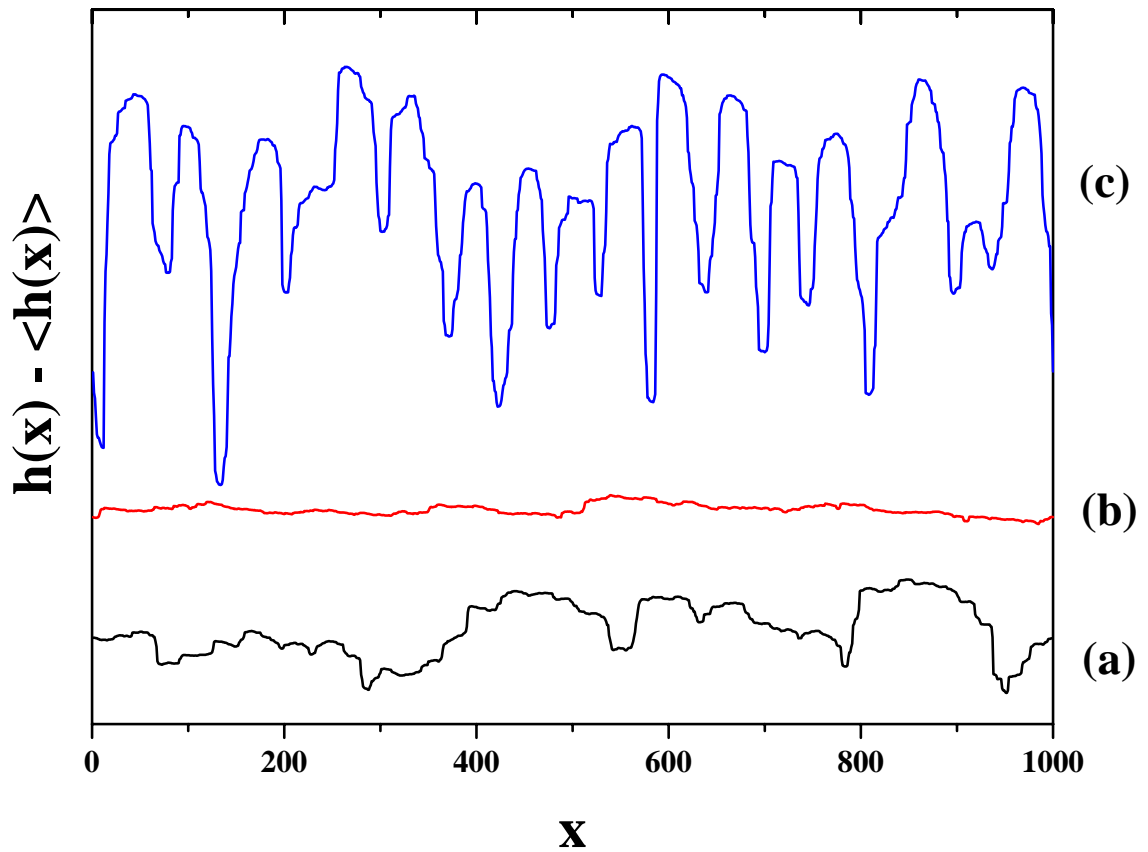


Figure 3.9: The morphologies of the WV-ES model when we set (a) $P_D = 1.0$ and $P_U = 1.0$, (b) $P_U = 0.5$, and $P_D = 1.0$, (c) $P_U = 1.0$ and $P_D = 0.5$. Case (a) corresponds with the original WV model, (b) corresponds with the negative ES barrier, and (c) is the WV-ES model.

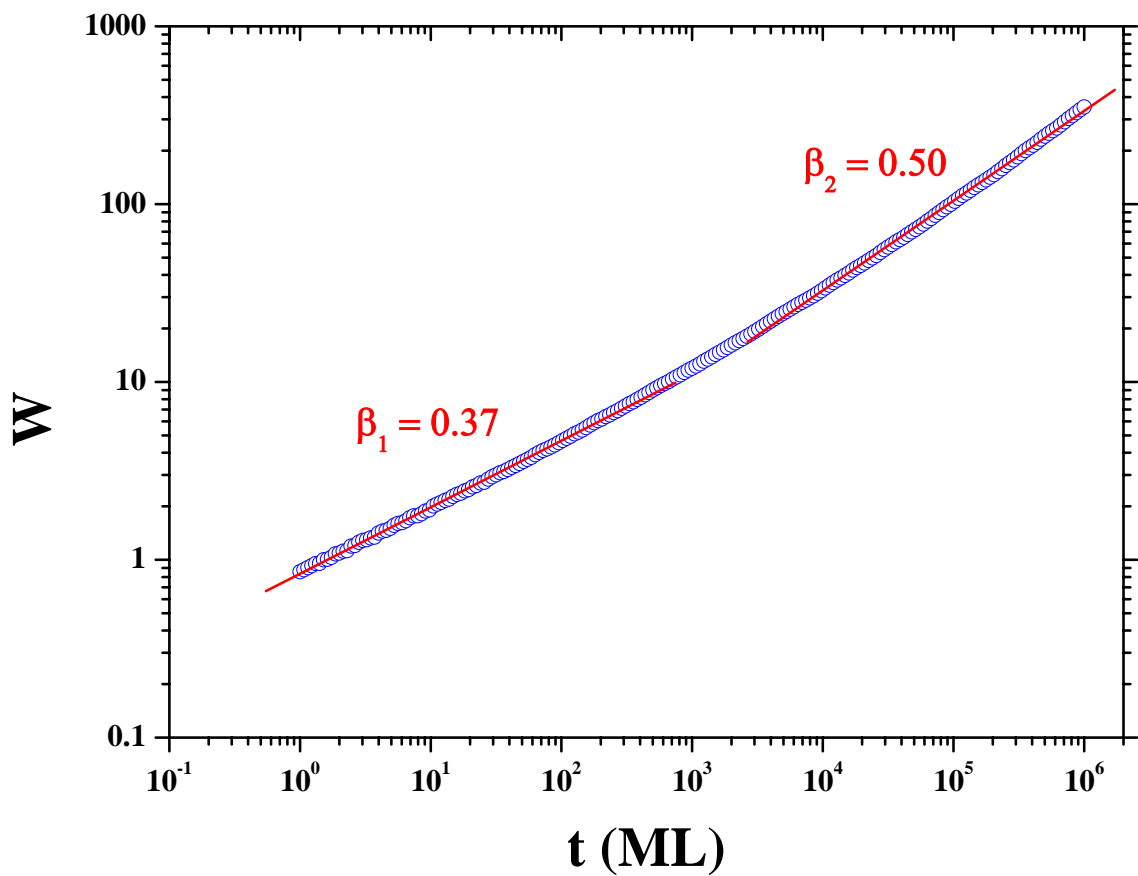


Figure 3.10: The surface width of the system with $L = 1000$, $P_U = 1.0$ and $P_D = 0.5$. We find the growth exponent crossover from $\beta_1 \approx 0.37$ to $\beta_2 \approx 0.50$ after the crossover time $t_c \approx 10^3$ ML.

growth exponent (denoted as β_1 in the figure) is approximately the same as in the original WV model, i.e. $\beta_1 \approx 0.37$. At longer time, however, the growth exponent (denoted as β_2) increases to $\beta_2 \approx 0.5$. From Fig 3.10, the crossover time (t_c) of the growth exponent is approximately at 10^3 ML. The crossover of β from $\beta \approx 0.37$ to $\beta \approx 0.5$ can be explained in the following way. In the early time ($t \ll t_c$) the whole substrate is still connected and the correlation length ξ follows the equation $\xi(t) \propto t^{1/z}$. During this time, mounds develop and coarsen through the diffusion process. By “coarsen” we mean a few small mounds combine and become one big mound. We can use the correlation function to detect the coarsening of mounds that we will explain in the next section. After the crossover time ($t \gg t_c$), the coarsening process drastically drops and the mounds almost stop growing laterally because grooves become too deep to be filled up. The newly deposited adatoms diffuse mostly on top of each existing mound and the mounds become steeper. At this point, each mound has very little interaction with other mounds on the surface and the correlation length is limited by the size of the mound. The “interaction” of mounds in this situation means each small mounds are coarsen to each other. It is as if in the $t \gg t_c$ regime the substrate is separated into pieces with almost no interaction between these pieces. This causes the growth exponent to increase and eventually $\beta \rightarrow 0.5$ just like in the RD model. It is interesting to note that this situation is independent of the strength of the ES barrier as long as the barrier is strong enough to induce mound formation. The difference is that t_c in a system with strong barrier is smaller than t_c in a weaker barrier system. This is shown in Fig. 3.11. In some very weak barrier systems, e.g. $P_D = 0.7$ and $P_D = 0.9$, we do not see the crossover to $\beta \approx 0.5$. It is possible that the barrier is not strong enough to induce mound and there is no such crossover, or there are some mound formation but t_c is larger than 10^6 ML in these cases. This is difficult to judge from the morphologies in Fig. 3.6 but it will be clearer when we discuss the correlation function in the next section.

Note that the value of $\beta \approx 0.5$ in WV-ES model is the same value as we found in the RD model but our WV-ES model behaves very differently from the

RD model (except for the trivial case when $P_U = P_D = 0$). In Fig. 3.12, we show that the saturation steady state exists in WV-ES model and the roughness exponent α , although very large, is still a finite value as shown in Fig. 3.13, while α is infinite in the RD model.

3.2 Correlation Function

Sometimes when we see the morphologies we cannot decide either there is mound formation on the surface or not. There is a tool that can be used to make that decision: the *correlation function* [2, 21, 22, 23], $G(r) = \langle h(\mathbf{x})h(\mathbf{x} + \mathbf{r}) \rangle_x$, introduced in Chapter 1. If we find an oscillation in the correlation function, it implies [2, 22, 23] that there are regular mound formation on the surface.

For this thesis, we start from the correlation function of the RD model. In Fig. 3.14, $G(r)$ is zero for all r with a small fluctuation. This means that there is no mound formation on the surface because $G(r)$ does not oscillate. When we calculate correlation function from the WV model, Fig. 3.4, we do not find any oscillation. This is shown in Fig. 3.15. So the WV morphology (Fig. 3.4) is just dynamical rough surface not a mounded surface. In the WV-ES systems, we have shown earlier that we find mounded morphologies when we fix the value of $P_U = 1.0$ and vary the values of P_D . In Fig. 3.16, we vary the values of P_D from 0.9 to 0.1 (where $P_D = 1.0$ corresponds to the original WV model), we find oscillations in the correlation function when $P_D \leq 0.7$, see Figs. 3.16(a)-(i). In Figs. 3.16(a) and (b), $G(r)$ for systems with $P_D \geq 0.8$ do not show any oscillation. We can deduce that there is no mound formation on the surfaces with large P_D (weak barriers). Note that the morphology of the system of $P_D = 0.8$ in Fig. 3.6 shows that mounds start forming however $G(r)$ plot for this system does not show any oscillation. This probably because the mounds seen in Fig. 3.6 when $P_D = 0.8$ are not regular enough since the barrier is not strong enough for $G(r)$ to oscillate.

Mounds properties can also be studied from the function $G(r)$. The average mound height is calculated from $\sqrt{G(r=0)}$ and the average mound radius is the

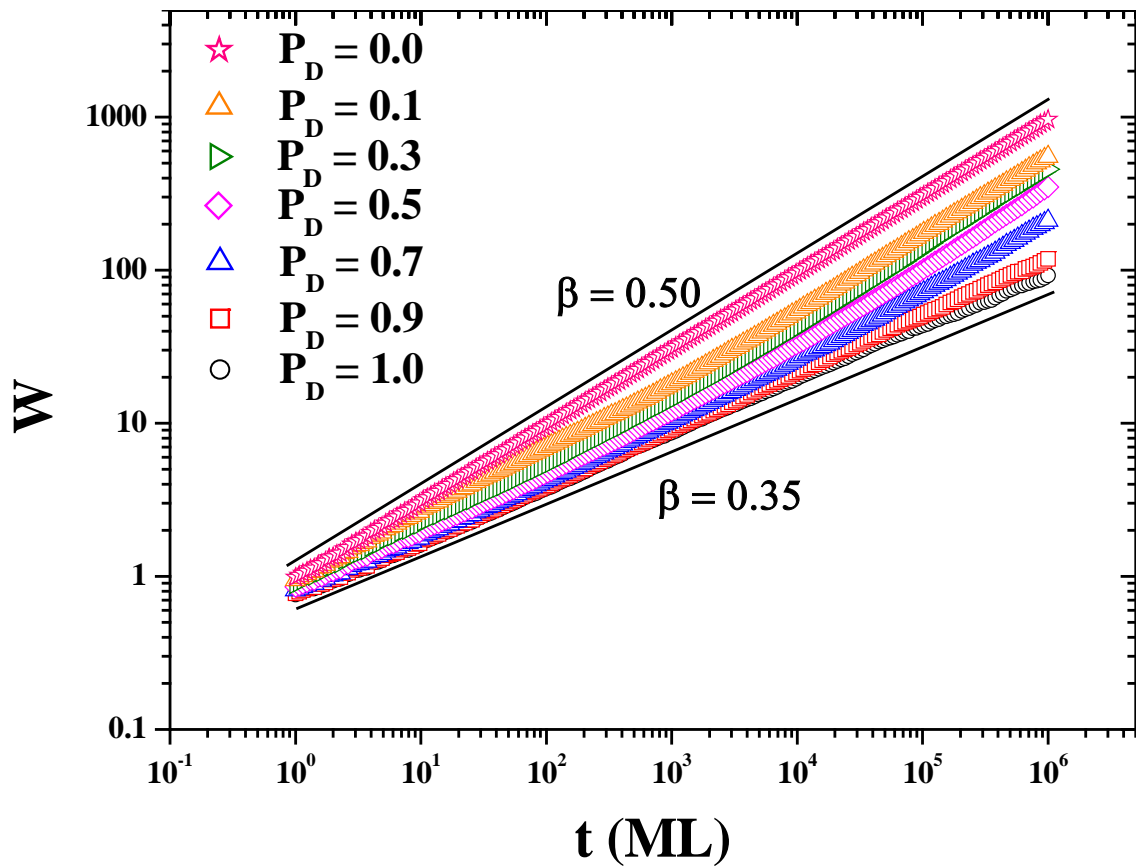


Figure 3.11: The surface width plot as a function of time in the system with $L = 1000$. We fixed $P_U = 1.0$ and varies the values of $P_D = 0.0, 0.1, 0.3, 0.5, 0.7, 0.9$, and 1.0 from top to bottom.

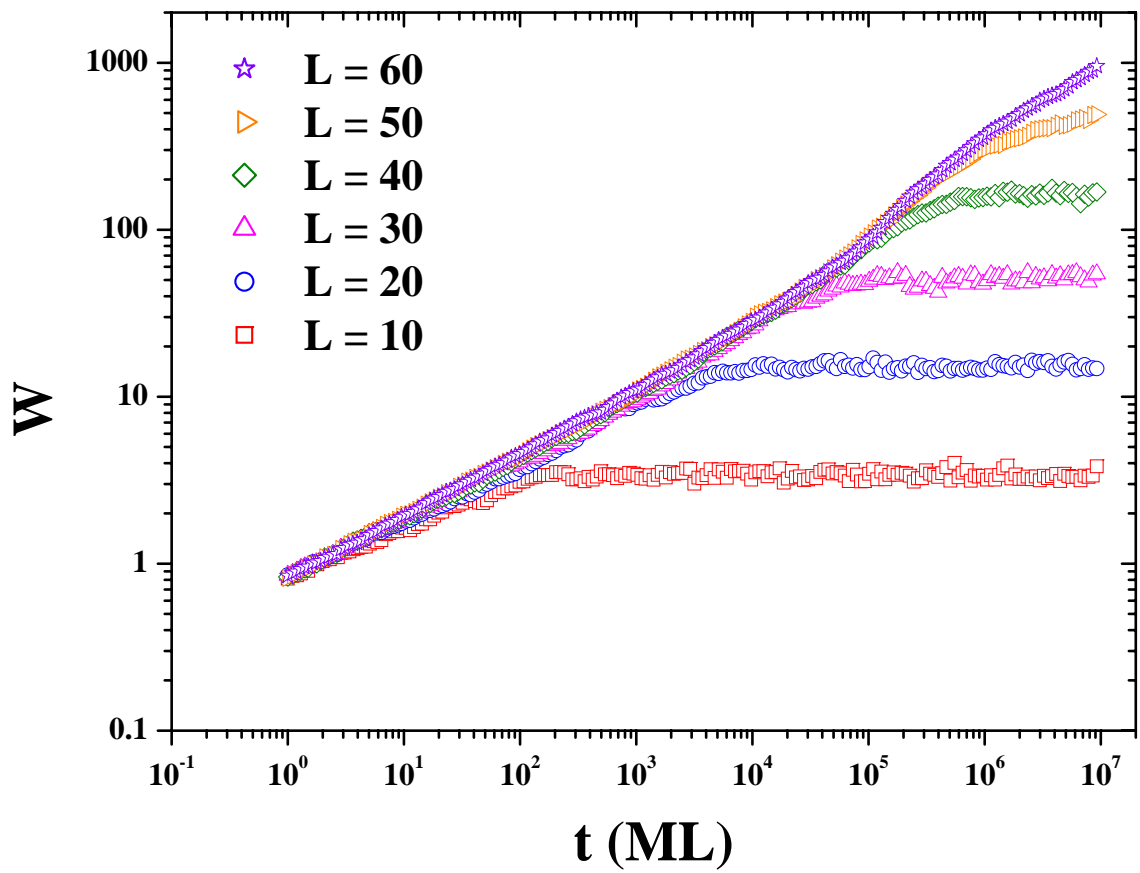


Figure 3.12: The W - t plot for our WV-ES model when we vary the substrate size $L = 10, 20, 30, 40$ and 50 , $P_U = 1.0$ and $P_D = 0.5$.

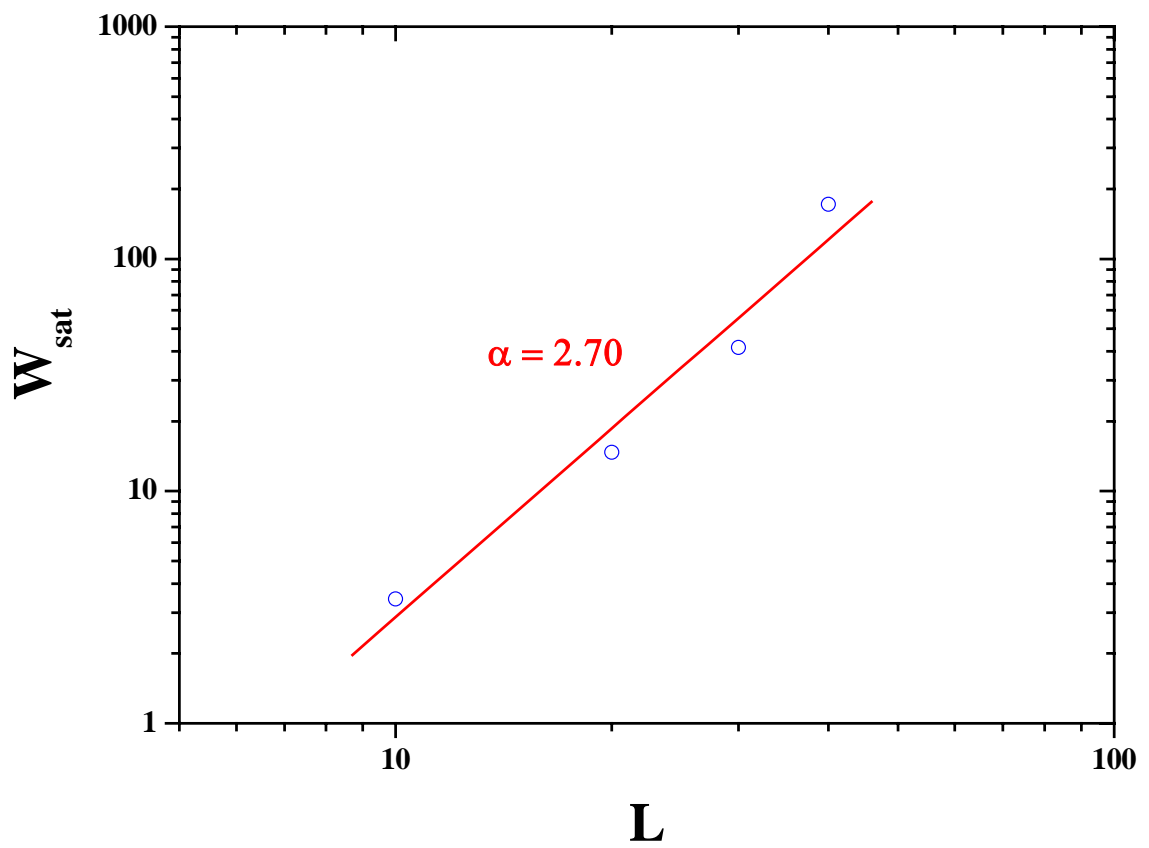


Figure 3.13: The calculation of the roughness exponent α in the WV-ES model. Here we obtained $\alpha \approx 2.70$.

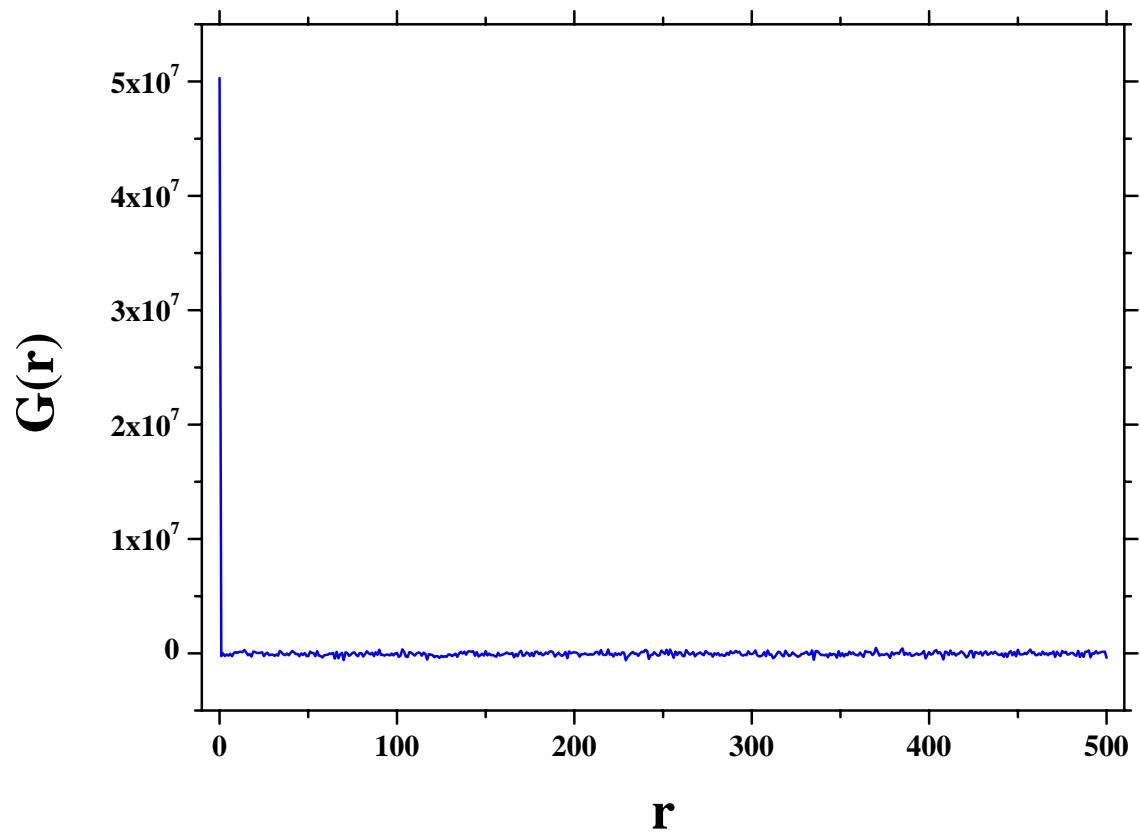


Figure 3.14: The correlation function of the RD model from the system of substrate size $L = 1000$ at time $t = 10^6$ ML.

distance of the first zero crossing of $G(r)$ as described in Chapter 1. From Fig. 3.16 we can see that the average mound height increases when P_D decreases while the average mound radius decreases when P_D decreases. This can be explained that the effect of a small value of P_D or a stronger barrier is to reduce the chance for a new adatom to hop down. Therefore, when a new adatom is deposited on top of each mound, it can diffuse only on each mound. The mound grows almost only in the vertical direction and becomes steeper with deeper grooves when P_D decreases. Furthermore, we can use $G(r)$ to detect the coarsening process by plotting $G(r)$ at different times. If the average mound radius calculated from the first zero crossing increases as the time increases, that means the coarsening still dominates in the growth process. However, when the average mound radius does not change in time, in another word, it remains constant as time increases, it means the coarsening process does not dominate in the growth process any more.

When we set the value of $P_U = P_D$ for all systems, the correlation function do not show any oscillation as in Fig. 3.17. Since the adatom has equals chance to hop in both directions, this is equivalent to no barrier in the system. So there is no mound formation on the surface in this case. In the cases of $P_U < P_D$, we do not see any oscillation either, see Fig. 3.18.

3.3 Particle Diffusion Current

In this section, we study the particle diffusion current [20] in the WV and WV-ES models in order to confirm whether these models belong to the EW universality class. As explained in Chapter 1, the particle diffusion current can help us determine the existence of the EW term, $\nabla^2 h$, in the continuum growth equation describing dynamic of the growth system.

Our results are summarized in Table 3.1 from a system of substrate size $L = 10^3$ and time $t = 10^6$ ML. The first result is the RD model. Since adatoms in this model are not allowed to diffuse, the particle current in this model is absolute

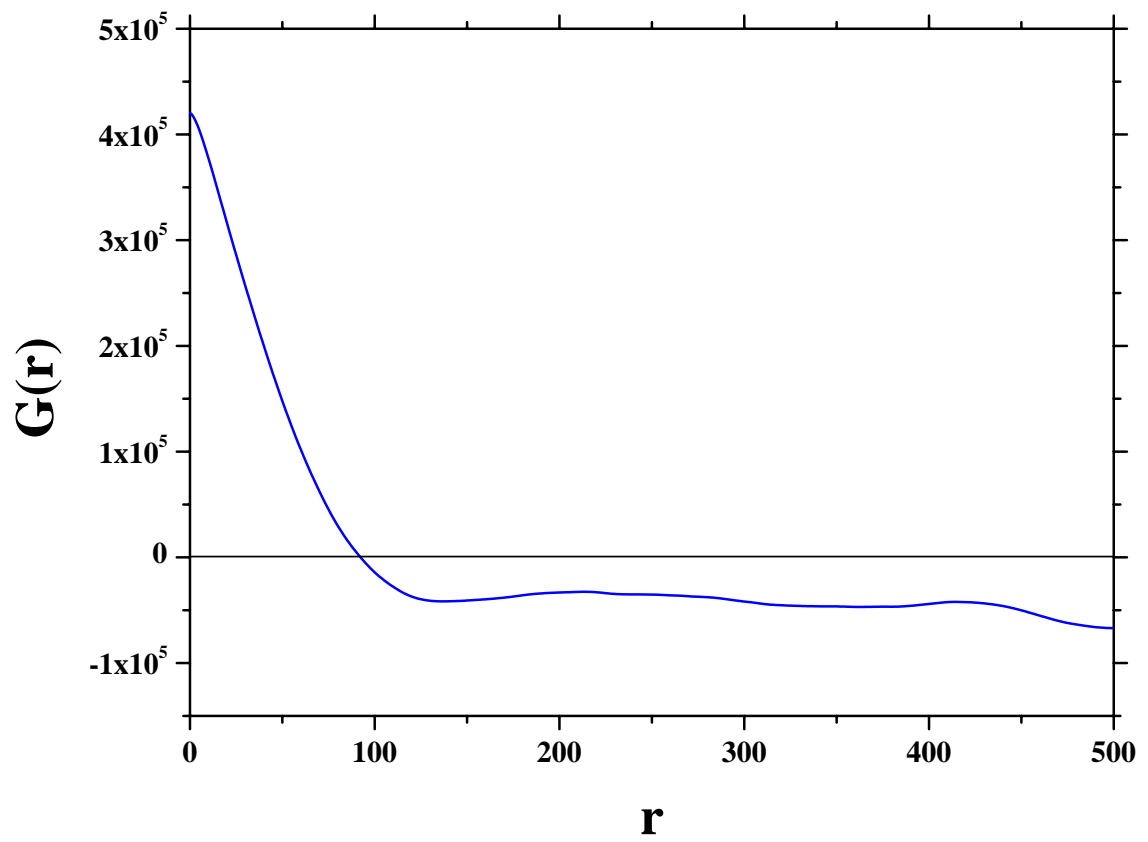


Figure 3.15: The correlation function of the WV model from the system of substrate size $L = 1000$ at time $t = 10^6$ ML.

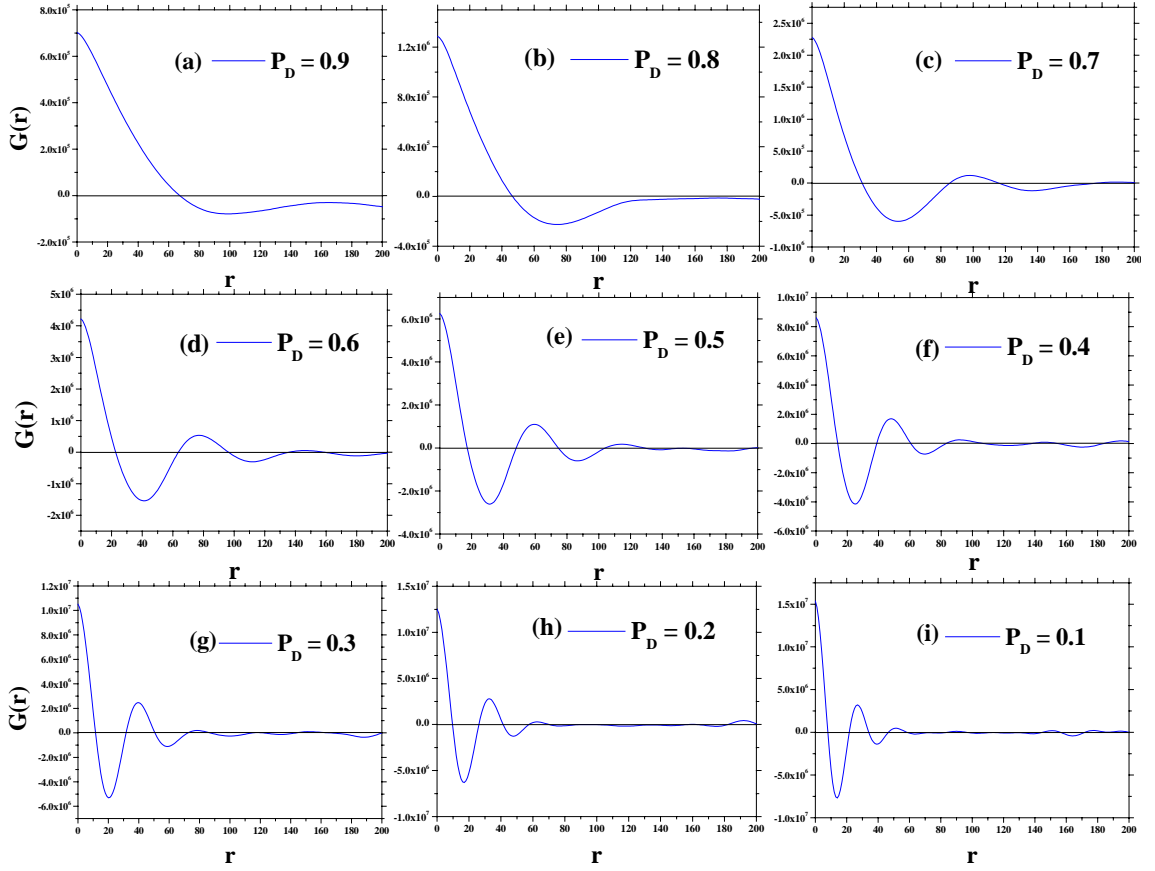


Figure 3.16: The correlation function of the WV-ES model from the system of substrate size $L = 1000$ at time $t = 10^6$ ML. We fix the value of $P_U = 1.0$ and vary the values of P_D from 0.9 to 0.1.

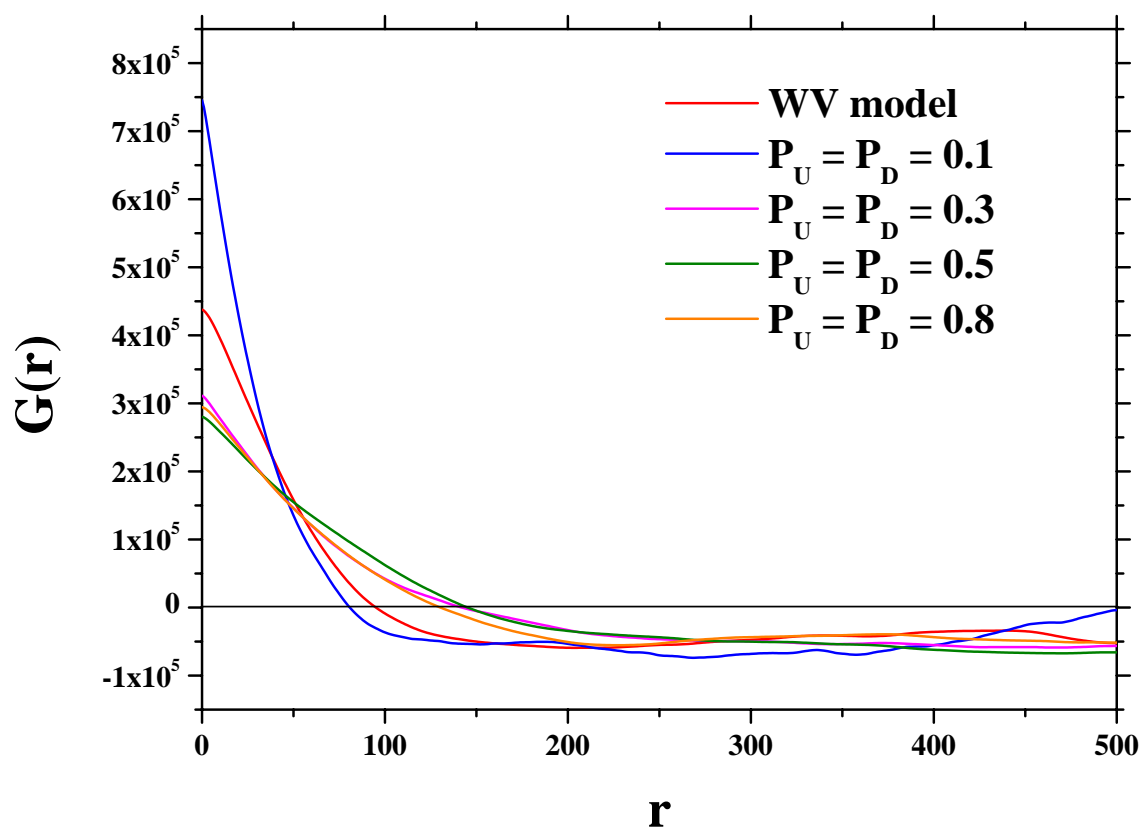


Figure 3.17: The correlation function of the WV-ES model in the case of $P_U = P_D$ from the system of substrate size $L = 1000$ at time $t = 10^6$ ML.

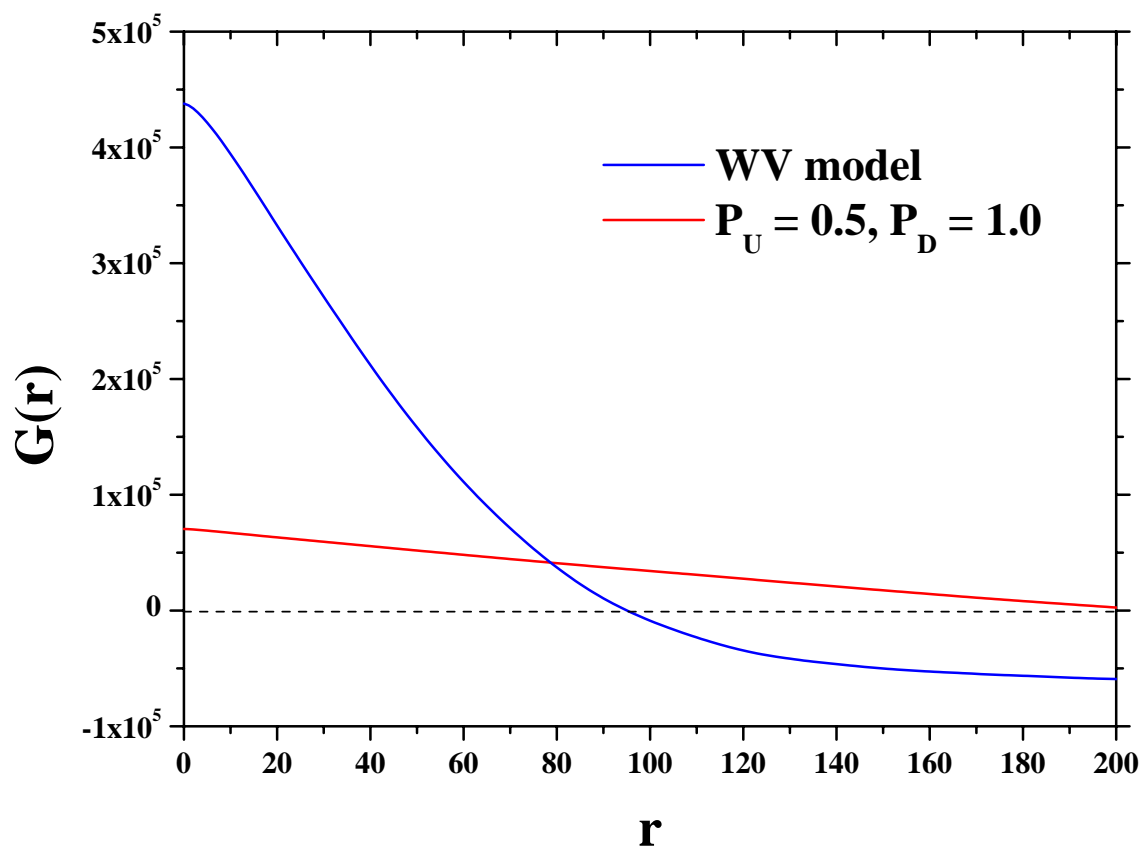


Figure 3.18: The correlation function of the WV-ES model in the cases of $P_U < P_D$ from the system of substrate size $L = 1000$ at time $t = 10^6$ ML.

zero, as shown in Fig 3.19. In the WV model, however, adatoms diffuse on the substrate and it is difficult to define “zero” current because the data fluctuates. To solve this problem, we study the WV model on a flat, i.e. untilt, substrate. The current obtained in this case is shown in Fig. 3.20. So we define “zero” current to be in the range between $\pm 5.0 \times 10^{-5}$. From the tilt substrate systems, the net current of the WV model is found to be *negative* or *downhill* as shown in Fig 3.21. This result confirms that WV model should follow the EW universality class asymptotically and it also implies that there is no mound formation on the WV surface. Our works agree with others [2, 20] that confirm the downhill current in 1+1 WV model.

| Model | current J at $\tan \theta$ equals to | | | |
|-----------------------|--|------------|------------|---------------|
| | 2 | 1 | 0.5 | 0 |
| RD | 0 | 0 | 0 | 0 |
| WV | -10^{-3} | -10^{-3} | -10^{-4} | $\pm 10^{-5}$ |
| WV-ES ($P_D = 0.5$) | $+10^{-3}$ | $+10^{-4}$ | $+10^{-4}$ | $\pm 10^{-5}$ |

Table 3.1: The particle diffusion current J of the discrete growth models.

For WV-ES model, we fixed $P_U = 1.0$ and then vary the values of P_D . We found that for $P_D = 1.0$ and 0.9 , the net current is negative while for $P_D \leq 0.8$ the net current is positive as shown in Fig 3.22. This indicates that, at $P_D = 1.0$ and 0.9 , the barrier is too weak to effect the system so the downhill current associating with the WV model has more influence on the system. The surface in this case is dynamical rough without mound formation. However, when $P_D \leq 0.8$ the ES barrier is strong and the uphill current associating with the ES barrier has more influence. In these cases we start to obtain mound formation on the surface (see Fig. 3.6 for the corresponding morphologies). But in the case of $P_D = 0.8$, we find the conflict between the correlation study and the particle current result, see Fig. 3.16 and Fig. 3.22. This may be because $P_D = 0.8$ is the boundary between mound formation surface and dynamical rough surface. So this value of P_D shows the conflict from the particle diffusion current and the correlation function.

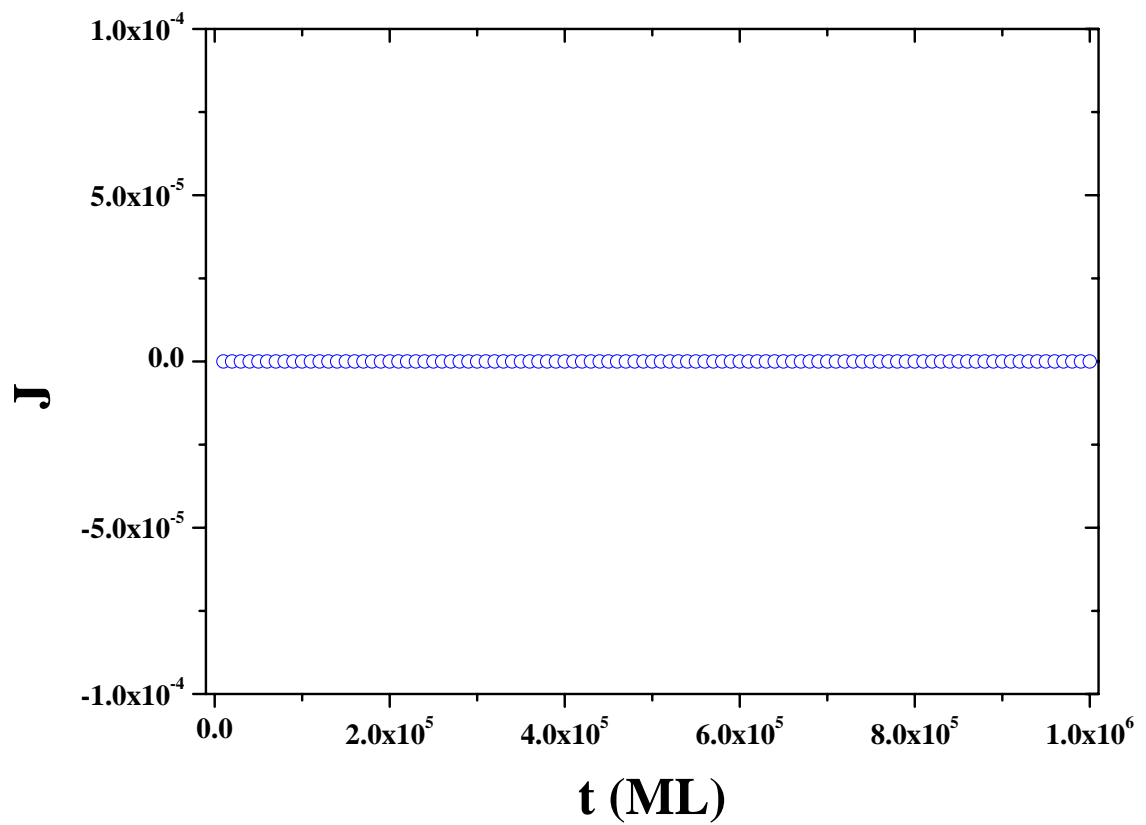


Figure 3.19: The particle diffusion current of the Random Deposition (RD) model. We obtained the zero current from the system of substrate size $L = 1000$ and $\tan \theta = 0.5$.

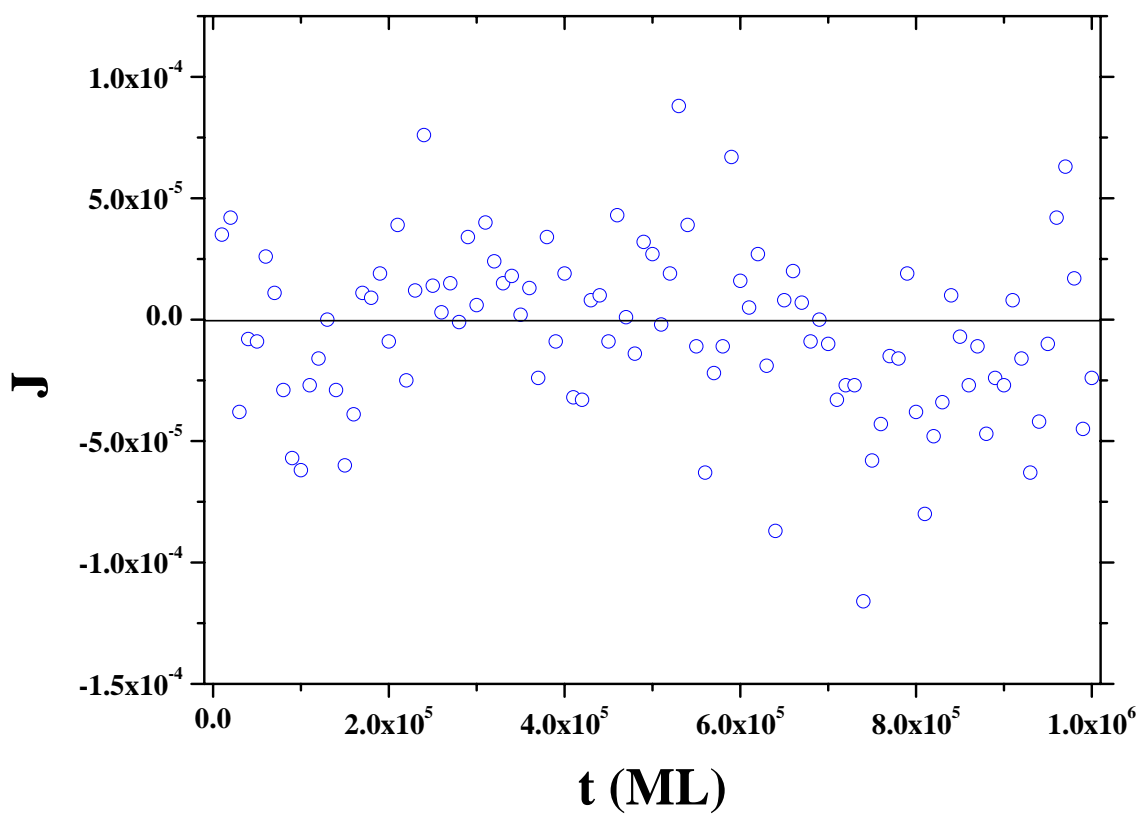


Figure 3.20: The particle diffusion current of the WV model with untilted substrate where we obtain the average zero current, $\pm 5.0 \times 10^{-5}$. This result comes from the system of substrate size $L = 1000$ and $\tan \theta = 0.5$.

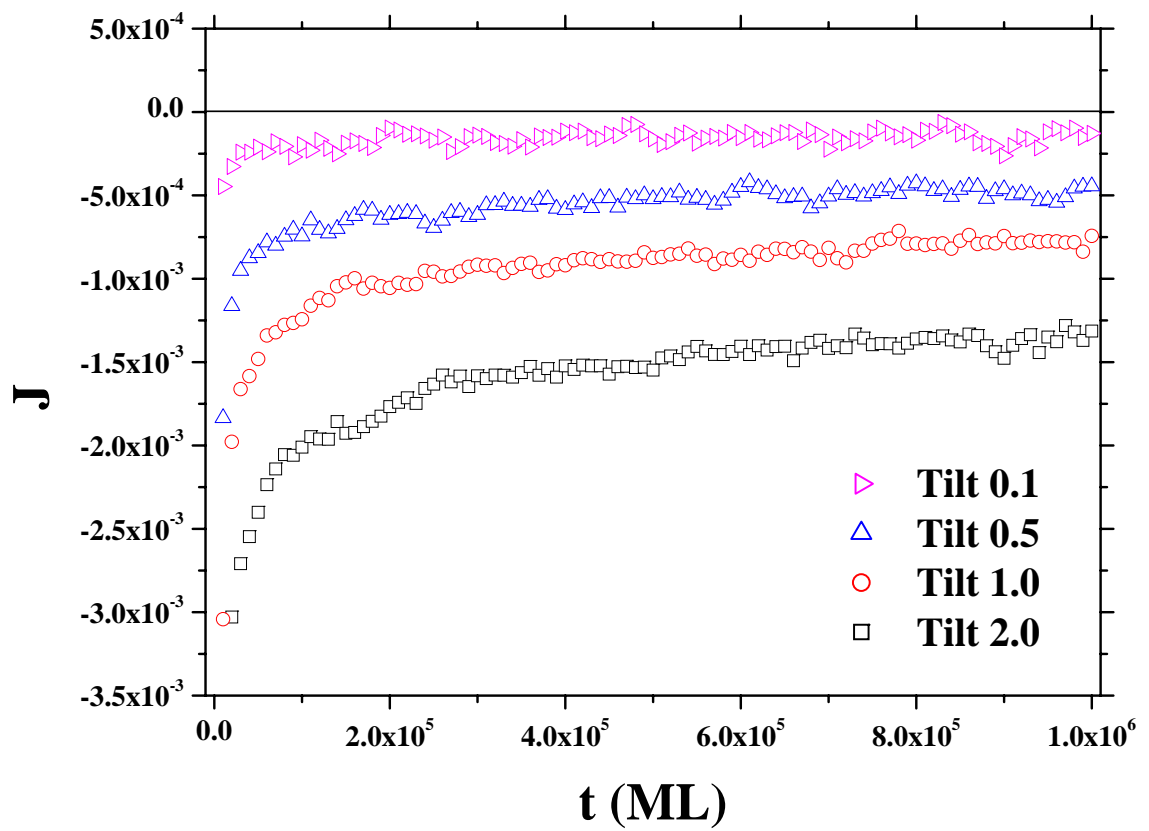


Figure 3.21: The particle diffusion current of the WV model with varying $\tan \theta$. We vary $\tan \theta = 0.1, 0.5, 1.0,$ and 2.0 from top to bottom. Here $L = 1000$.

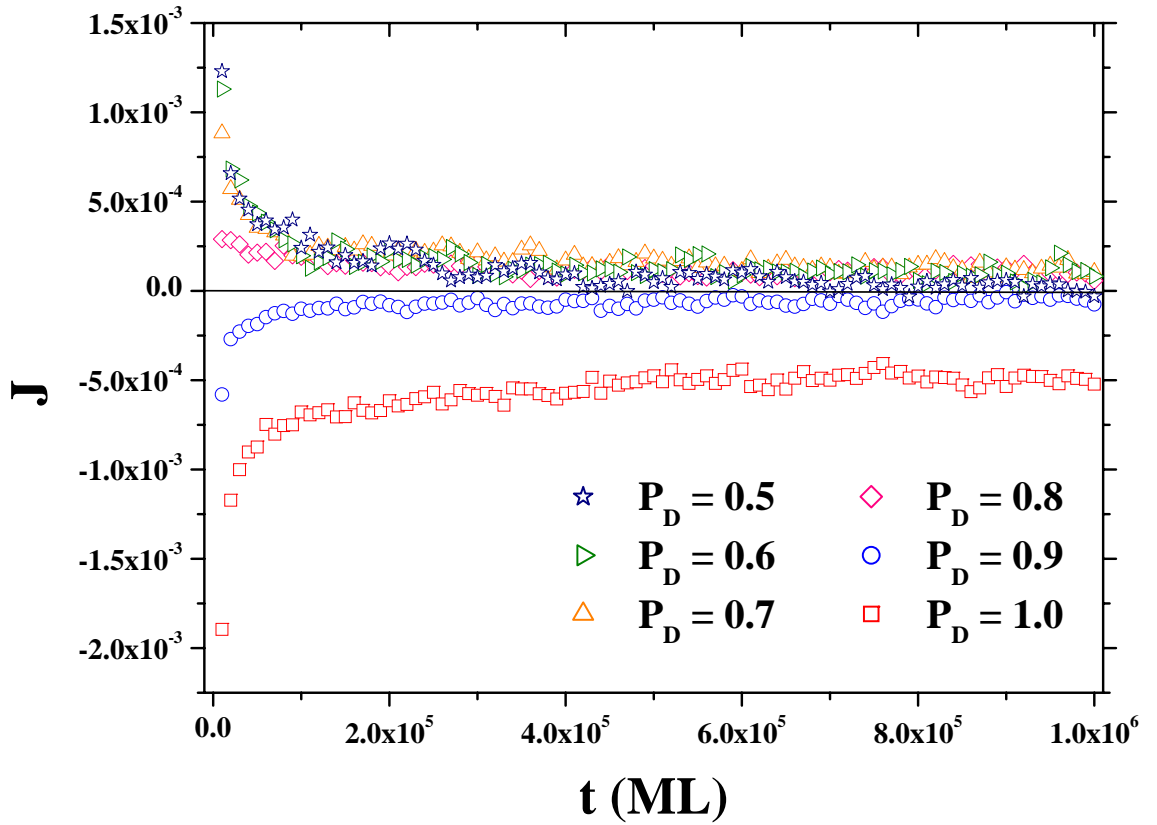


Figure 3.22: The particle diffusion current of the WV-ES model where we fix $P_U = 1.0$ and vary $P_D = 0.5$ to 1.0 with $\tan \theta = 0.5$. These results come from the systems of substrate size $L = 1000$.

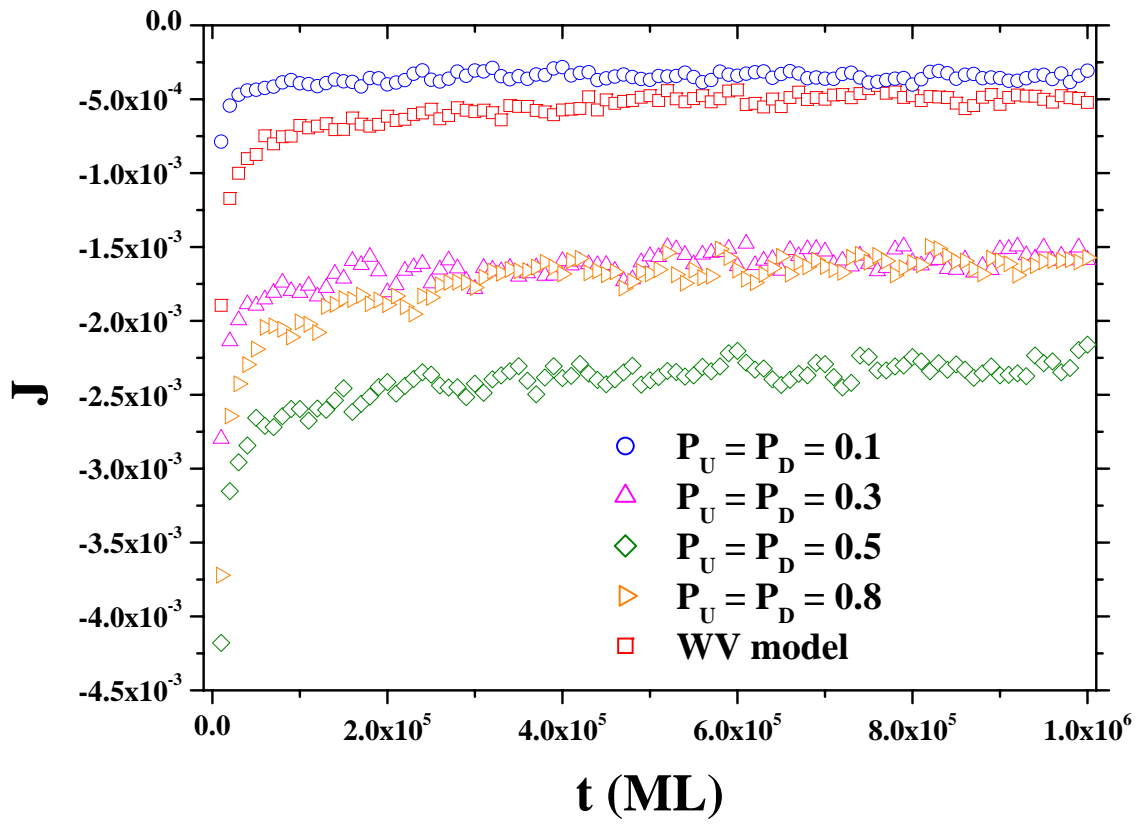


Figure 3.23: The particle diffusion current of the WV-ES model in the case of $P_U = P_D$ with $\tan \theta = 0.5$. Here $L = 1000$.

In the case of $P_U = P_D$, we find the downhill current in every values of P_D as shown in Fig. 3.23. These current results agree with all our results (morphologies and surface width) and confirm that when $P_U = P_D$ the system behaves in the same way as the original WV model.

3.4 Growth Equation

Since all three exponents (α , β , z) from our simulation, the WV model in 1+1 dimensions seem to match the linear fourth order growth equation (Eq. (1.20)), so the linear fourth order term, $\nabla^4 h$, must be in the continuum growth equation. However, from the characteristic of the morphology, the up-down symmetry is broken [2, 3, 19] so a linear equation cannot describe the system and it seems the nonlinear fourth order term ($\nabla^2(\nabla h)^2$) is also presented in the continuum growth equation. Our particle diffusion current in the previous section shows a downhill current for the WV model which implies that the linear second order term (the EW term, $\nabla^2 h$) must be in the continuum growth equation too. So from all our results, the continuum growth equation describing the WV model in 1+1 dimensions should be in the form of

$$\frac{\partial h}{\partial t} = \nu_2 \nabla^2 h - \nu_4 \nabla^4 h + \lambda_{22} \nabla^2 (\nabla h)^2 + \eta(x, t). \quad (3.1)$$

With this equation, the WV simulation results should show statistical properties that belong to the $\nabla^4 h$ and $\nabla^2(\nabla h)^2$ terms and the eventual crossover to the behavior of the $\nabla^2 h$ term asymptotically. But due to the limit of computer resources and time constraints, we cannot carry out our simulations long enough to see this crossover. All our simulations still produce the critical exponents which belong to the MH equation, $\nabla^4 h$, as shown in Table 1.1. The only evidence of the $\nabla^2 h$ term is the downhill particle current in the previous section.

When we add the ES barrier into the WV model, all of our WV-ES model results do not agree with any universality class discussed in Chapter 1. The morphologies show mounds (or instability), the surface width has a crossover to

$\beta \rightarrow 0.5$, and the particle current is uphill. It is difficult to form a continuum equation to describe unstable growth like the WV-ES case. The only thing we can say is that the $\nabla^2 h$ term should be included in the equation with $\nu_2 < 0$ to reflect the instability.

Chapter IV

Conclusions

In our works, the results obtained from simple nonequilibrium growth model which is used to study the *ideal* molecular beam epitaxy (MBE) growth. Our study is based on 1+1 dimensional growth and under the solid-on-solid (SOS) constraints. The Wolf-Villain (WV) model [3] is the main model that we are interested in for the study of MBE growth. In real MBE growth, the existence of a potential barrier, known as the ES barrier [6, 7, 8], is seen experimentally. The barrier prevents an adatom from diffusing down to the lower terrace. Our main interest is to study the effects of the ES barrier on the WV model.

For the WV model, we start with the study of scaling properties. We find the growth exponent $\beta \approx 0.37$, the roughness exponent $\alpha \approx 1.40$ and the dynamical exponent $z = \alpha/\beta \approx 4$. These results agree with the Mullins-Herring (MH) universality class [14, 15]. However, the true asymptotic universality class of the WV model is the Edward-Wilkinson (EW) universality class [13]. In our simulations, we cannot reach the asymptotic time and find the asymptotic scaling properties of the WV model because of the limitation of our computer facilities. The downhill particle diffusion current is obtained for the WV model and confirms the EW behavior.

After we apply the ES barrier into the WV model (WV-ES model) by modify its diffusion rule. The ES barrier induces mound formation on the surface. In this situation, we confirm mound formation by using the particle diffusion current and the correlation function. The particle current is uphill and the correlation function oscillates from the WV-ES model. For the scaling properties of the WV-ES model, the growth exponent (β) in early time ($t \ll t_c \approx 10^3$ ML) approaches the same β as obtained from the original WV model. After $t \gg t_c$, β increases and approaches 0.5. This behavior does not depend on the strength of the ES barrier, which is

defined by the ratio of P_U/P_D , as long as it is strong enough to induce mound. We find that when $P_D \geq 0.9$, the barrier is too weak and the effect of downhill current of the original WV model still influence the system and there is no mound formation. When $P_D = 1.0$, it corresponds with the original WV model. When $P_D \leq 0.7$ the particle diffusion current shows the uphill current and the correlation function oscillates. This implies that there are mound formation on the surface and their results are corresponding to each other. But when $P_D = 0.8$, there is a conflict between correlation function and the particle diffusion current. This may be due to at this value of P_D is the boundary between mound formation surface and dynamical rough surface. So at this value of P_D , it shows the confliction between these tools. Furthermore, the average mound height increases when the strength of the ES barrier increases (P_D decreases) while the average mound radius decreases when the barrier becomes stronger.

From our results, the continuum growth equation of the WV model in 1+1 dimensions is

$$\frac{\partial h}{\partial t} = \nu_2 \nabla^2 h - \nu_4 \nabla^4 h + \lambda_{22} \nabla^2 (\nabla h)^2 + \eta(x, t). \quad (4.1)$$

We should note here that the uphill current and the oscillatory correlation function can help us to detect mounds, but they cannot help us determine the cause of the mounded surface. Because there are other possible causes for mounds too [16, 31, 32]. So when seeing mounded surfaces, we should not rush to conclude that the ES barrier is the cause. But for our study, we can deduce that mound formations on the surface come from the effect of the ES barrier. In another word, the ES barrier is the cause of mound formation on the surface in our study.

For future work, we can make the model more realistic by studying growth on two dimensional substrates. Furthermore, we may relax the SOS constraints from the model. The effects of the substrate temperature can make each adatom hops more than once in the simulation. It will be very complicated if we apply all effects above into the model, and it will require more simulation time. But the modified model will be more realistic than the original WV model studied here.

References

- [1] A.-L. Barabási and H. E. Stanley, *Fractal Concepts in Surface Growth*, Cambridge University Press, Cambridge, 1995.
- [2] P. Punyindu, *Understanding Kinetic Surface Roughening Using Local, Discrete, Nonequilibrium Growth Models.*, Doctoral Dissertation, Faculty of the Graduate School, University of Maryland, 2000.
- [3] D. E. Wolf and J. Villain, *Europhys. Lett.* **13**,389 (1990).
- [4] S. Das Sarma and P. I. Tamborenea, *Phys. Rev. Lett.* **66**, 325 (1991).
- [5] P. I. Tamborenea and S. Das Sarma, *Phys. Rev. E* **48**, 2575 (1993).
- [6] G. Ehrlich and F. G. Hudda, *J. Chem. Phys.* **44**, 1039 (1966).
- [7] R. L. Schwoebel and E. J. Shipsey, *J. Appl. Phys.* **37**, 3682 (1966).
- [8] K. Kyuno and G. Ehrlich, *Surf. Sci.* **394**, L179 (1997).
- [9] F. Family and T. Vicsek, *J. Phys. A* **18**, L75 (1985).
- [10] S. Das Sarma, arXiv:cond-mat/9705118 (1997).
- [11] M. Kardar, G. Parisi and Y.-C. Zhang, *Phys. Rev. Lett.* **56**, 889 (1986).
- [12] J. R. Leith, *Sign. Proc.* **83**, 2397 (2003).
- [13] S. F. Edwards and D. R. Wilkinson, *Proc. R. Soc. London, Ser. A* **381**, 17 (1982).
- [14] C. Herring, *J. Appl. Phys.* **21**, 301 (1950).
- [15] W. W. Mullins, *J. Appl. Phys.* **28**, 333 (1957).
- [16] Z. W. Lai and S. Das Sarma, *Phys. Rev. Lett.* **66**, 2348 (1991).

- [17] J. M. Kim and S. Das Sarma, Phys. Rev. E **51**, 1889 (1995).
- [18] S. Das Sarma and R. Kotlyar, Phys. Rev. E. **50**, R4275 (1994).
- [19] S. Das Sarma, C. J. Lanczycki, R. Kotlyar and S. V. Ghaisas, Phys. Rev. E **53**, 359 (1996).
- [20] J. Krug, M. Plischke, and M. Siegert, Phys. Rev. Lett. **70**, 3271 (1993).
- [21] S. Das Sarma and P. Punyindu, Surf. Sci. **424**, L339 (1999).
- [22] S. Das Sarma, P. Punyindu and Z. Toroczkai, Surf. Sci. **457**, L369 (2000).
- [23] P. P. Chatrathorn, Z. Toroczkai and S. Das Sarma, Phys. Rev. B **64**, 205407 (2001).
- [24] W. H. Press, S. A. Teukolsky, W. T. Vetterling, B. P. Flannery, *Numerical Recipes in C, The Art of Scientific Computing*, 2nd Ed. (Acrobat Ed.), Numerical Recipes Books On-Line, Cambridge University Press, 1992. Available from: <http://lib-www.lanl.gov/numerical/bookcpdf.html>
- [25] J. Villain, J. Phys. (France) I **1**, 19 (1991).
- [26] P. Šmilauer, M. Kotrla, Phys. Rev. B **49**, 5769 (1994).
- [27] D. D. Vvedensky, Phys. Rev. E **68**, 010601(R) (2003).
- [28] Z. F. Huang and B.-L. Gu, Phys. Rev. E **54**, 5935 (1996).
- [29] Y. Kim and S. Y. Yoon, Phys. Rev. E **65**, 041609 (2002).
- [30] M. H. Xie, S. Y. Leung and S. Y. Tong, Surf. Sci. **515**, L459 (2002).
- [31] M. V. Ramana Murty and B. H. Cooper, Surf. Sci. **539**, 91 (2003).
- [32] J. G. Amar and F. Family, Phys. Rev. Lett. **77**, 4584 (1996).

Vitae

Mr. Rachan Rangdee was born on 19 December 1977 in Chaing Rai, Thailand. He received his Bachelor degree of Science in Physics from Naresuan University in 2000.

Conference Presentations:

- 2004 Rachan Rangdee, Patcha Chatraphorn, “Wolf-Villain Model with Ehrlich-Schwoebel Barrier”, *The 12th Science Seminar 2004*, Faculty of Science, Chulalongkorn University (March 18-19, 2004): PH-3
- 2004 Rachan Rangdee, Patcha Chatraphorn, “A Study of Wolf-Villain Model with Ehrlich-Schwoebel Barrier”, *The 8th Annual National Symposium on Computational Science and Engineering (ANSCSE8)*, Suranaree University of Technology (July 21-23, 2004): CP-003
- 2004 Rachan Rangdee, Patcha Chatraphorn, “Ehrlich-Schwoebel barrier in a model for MBE growth”, *The 4th National Symposium on Graduate Research*, Lotus Pang Suankaew Hotel, Chiang Mai (August 10-11, 2004): O-ST-59